MycoKeys 95: 131–162 (2023)
doi: 10.3897/mycokeys.95.98125
https://mycokeys.pensoft.net

RESEARCH ARTICLE

A peer-reviewed open-access journal
MycoKeys
Launched to accelerate biodiversity research

# Segregation of the genus *Parahypoxylon* (Hypoxylaceae, Xylariales) from *Hypoxylon* by a polyphasic taxonomic approach

Marjorie Cedeño-Sanchez[1,2*], Esteban Charria-Girón[1,2*], Christopher Lambert[1,2,3], J. Jennifer Luangsa-ard[4], Cony Decock[5], Raimo Franke[6], Mark Brönstrup[6,7], Marc Stadler[1,2]

**1** *Dept. Microbial Drugs, Helmholtz Centre for Infectiion Research, Inhoffenstrasse 7, 38124 Braunschweig, Germany* **2** *Institute of Microbiology, Technische Universität Braunschweig, Spielmannstraße 7, 38106 Braunschweig, Germany* **3** *Division of Molecular Cell Biology, Zoological Institute, Technische Universität Braunschweig, Spielmannstrasse 7, 38106 Braunschweig, Germany* **4** *National Center for Genetic Engineering and Biotechnology (BIOTEC), 113 Thailand Science Park, Phaholyothin Road, Klong Luang, Pathumthani 12120, Thailand* **5** *Mycothéque de l' Universite catholique de Louvain (BCCM/MUCL), Place Croix du Sud 3, B-1348 Louvain-la-Neuve, Belgium* **6** *Department of Chemical Biology, Helmholtz Centre for Infection Research, Partner site Hannover/Braunschweig, Inhoffenstrasse 7, 38124 Braunschweig, Germany* **7** *German Center for Infection Research (DZIF), Site Hannover-Braunschweig, 38124 Braunschweig, Germany*

**Corresponding author:** Marc Stadler (marc.stadler@helmholtz-hzi.de)

**Academic editor:** Andrew Miller | Received 28 November 2022 | Accepted 31 January 2023 | Published 20 February 2023

**Citation:** Cedeño-Sanchez M, Charria-Girón E, Lambert C, Luangsa-ard JJ, Decock C, Franke R, Brönstrup M, Stadler M (2023) Segregation of the genus *Parahypoxylon* (Hypoxylaceae, Xylariales) from *Hypoxylon* by a polyphasic taxonomic approach. MycoKeys 95: 131–162. https://doi.org/10.3897/mycokeys.95.98125

## Abstract

During a mycological survey of the Democratic Republic of the Congo, a fungal specimen that morphologically resembled the American species *Hypoxylon papillatum* was encountered. A polyphasic approach including morphological and chemotaxonomic together with a multigene phylogenetic study (ITS, LSU, *tub2*, and *rpb2*) of *Hypoxylon* spp. and representatives of related genera revealed that this strain represents a new species of the Hypoxylaceae. However, the multi-locus phylogenetic inference indicated that the new fungus clustered with *H. papillatum* in a separate clade from the other species of *Hypoxylon*. Studies by ultrahigh performance liquid chromatography coupled to diode array detection and ion mobility tandem mass spectrometry (UHPLC-DAD-IM-MS/MS) were carried out on the stromatal extracts. In particular, the MS/MS spectra of the major stromatal metabolites of these species indicated the production of hitherto unreported azaphilone pigments with a similar core scaffold to the cohaerin-type metabolites, which are

* These authors contributed equally to this work.

Copyright *Marjorie Cedeño-Sanchez et al.* This is an open access article distributed under the terms of the Creative Commons Attribution License (CC BY 4.0), which permits unrestricted use, distribution, and reproduction in any medium, provided the original author and source are credited.

exclusively found in the Hypoxylaceae. Based on these results, the new genus *Parahypoxylon* is introduced herein. Aside from *P. papillatum,* the genus also includes *P. ruwenzoriense* **sp. nov.**, which clustered together with the type species within a basal clade of the Hypoxylaceae together with its sister genus *Durotheca*.

**Keywords**

Ascomycota, metabolite annotation, one new genus, one new species, phylogeny, polythetic taxonomy, Xylariales

## Introduction

The genus *Hypoxylon* Bull. 1791 remains one of the largest in the Xylariales, even after a turbulent taxonomic history, during which its generic concept has changed drastically. Its early taxonomic history has been reviewed in great detail by Ju and Rogers (1996). Therefore, we largely refer to this monograph for the taxonomic treatments that occurred in the 19th and early 20th century.

The first world monograph of *Hypoxylon* by Miller (1961) was mainly based on stromatal morphology and ascal micromorphology. He recognized four sections (*Hypoxylon*, *Annulata*, *Applanata* and *Papillata*, the latter of which was further subdivided into two subsections, *Papillata* and *Primocinerea*). Ju and Rogers (1996) then restricted *Hypoxylon* to sections *Hypoxylon* and *Annulata*, and included several species of section *Papillata* in their emended section *Hypoxylon*. The main criteria for this taxonomic change were the presence of stromatal pigments and a nodulisporium-like anamorph. Many of the species in sections *Applanata* and *Papillata* sensu Miller (1961) do not show the latter mentioned features and were accommodated in other genera (e.g., *Biscogniauxia*, *Nemania*, *Whalleya*), which were later transferred to different families (Wendt et al. 2018). For their current classification, we refer to Hyde et al. (2020).

With the advent of molecular phylogenetic studies, and chemotaxonomy as an additional tool, the taxonomic concepts of *Hypoxylon* and other stromatic genera of the Xylariales have been further refined. The holomorphic concepts developed by Ju and Rogers, as well as other mycologists who put more emphasis on the anamorphic characters than on stromatal and ascospore morphology, have largely been confirmed. Hsieh et al. (2005) used protein-coding genes of a large number of representative taxa to resolve the phylogeny of *Hypoxylon* s. lat., which resulted in the recognition of the genus *Annulohypoxylon*. The composition of the latter genus was then equivalent to that of sect. *Annulata* sensu Ju and Rogers (1996). Notably, a parallel approach to establish a phylogeny based on ITS nrDNA sequences resulted in a very low resolution of the hypoxyloid taxa (Triebel et al. 2005). Later studies revealed that a multi locus phylogeny involving both protein-coding genes and rDNA are suitable to achieve a sufficient phylogenetic resolution within *Hypoxylon* and its allies (Kuhnert et al. 2014b, 2015, 2017a; Sir et al. 2015) in scope of a polythetic concept. Concurrent chemotaxonomic studies have aided in establishing correlations between the genotypes and the phenotypes of these pyrenomycetes. Their stromatal pigments, as well as certain secondary metabolites of their mycelial cultures, turned out to be informative for

taxonomic segregation at the species or even genus level (cf. Helaly et al. 2018; Becker and Stadler 2021).

Based on the above accomplishments, Wendt et al. (2018) proposed a rearrangement of the families of the stromatic Xylariales, as well as the further segregation of genera from the mainstream of *Hypoxylon*. The Hypoxylaceae were resurrected to accommodate *Hypoxylon* and its closely related allies, and the Xylariaceae were restricted to the genera with geniculosporium-like anamorphs, which had already been recognized as phylogenetically distinct in earlier studies (e.g., Hsieh et al. 2010). *Annulohypoxylon* was further subdivided and largely restricted to those species that have ostiolar rings and do not produce cohaerin-type azaphilones. The genus *Jackrogersella* was erected to accommodate those species of *Annulohypoxylon* sensu Hsieh et al. (2005) that produce the aforementioned compounds and have papillate ostioles without rings. In addition, the genus *Pyrenopolyporus* was erected for species of *Hypoxylon* sensu Ju and Rogers (1996) that have massive stromata, long tubular perithecia, contain naphthopyrones in their stromata and (where this is known) produce a characteristic virgariella-like anamorph. A follow-up study by Lambert et al. (2019) provided evidence that the species of the *H. monticulosum* complex differ from *Hypoxylon* by the production of antifungal sporothriolides in culture. In addition, these fungi also lack the typical stromatal pigments of *Hypoxylon* (Fig. 1) and appear in a basal clade in the molecular phylogeny. The genus *Hypomontagnella* was therefore introduced to accommodate them.

The genus *Hypoxylon* in the current sense still appears heterogeneous and paraphyletic in the recently established phylogenies, also because its type species, *H. fragiforme* clustered in a relatively small clade comprising only a few species such as *H. howeanum*, *H. ticinense* and *H. rickii* (Wendt et al. 2018; Lambert et al. 2021). The latter species have in common that their stromatal pigments are of the mitorubrin type.

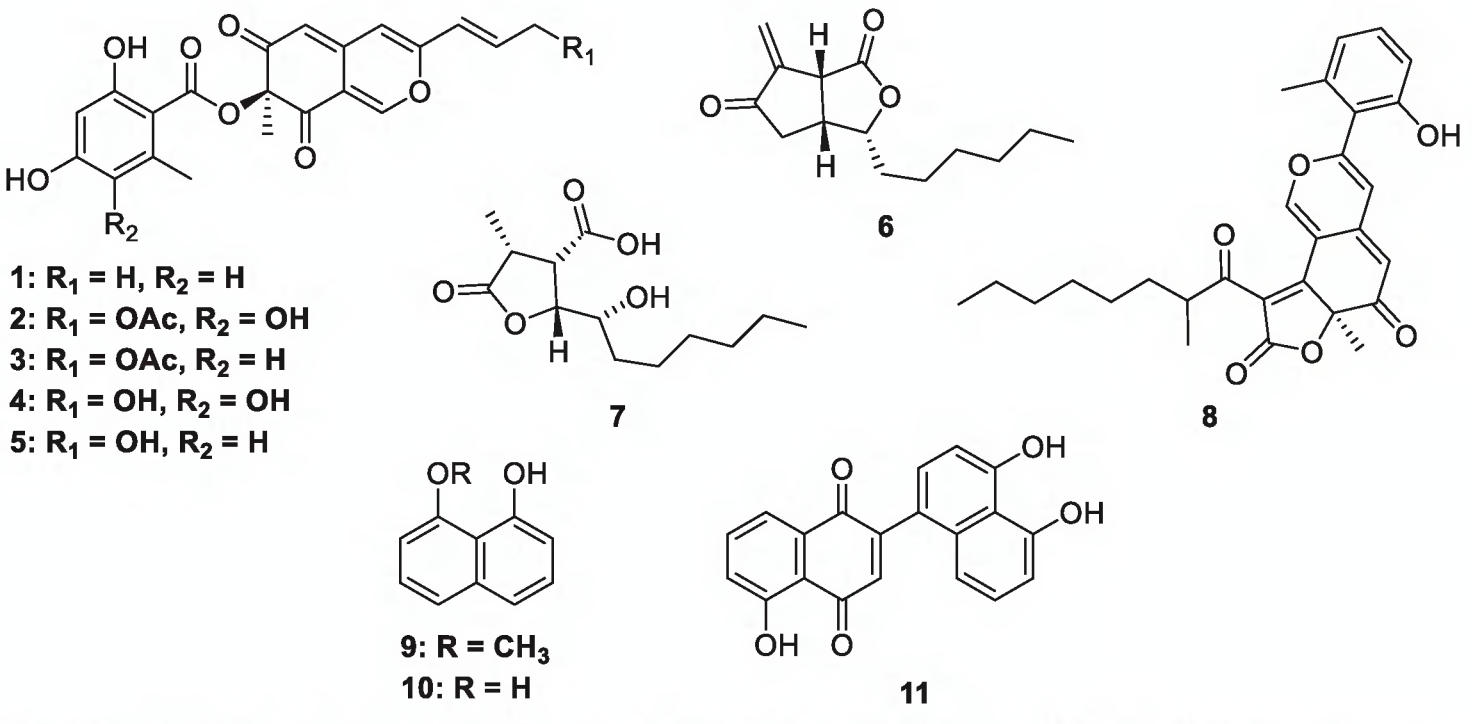


**Figure 1.** Characteristic stromatal pigments and other secondary metabolites of *Hypoxylon* species. (+)-mitorubrin (**1**); (+)-6″-hydroxymitorubrinol acetate (**2**); (+)-mitorubrinol acetate (**3**); (+)-6″-hydroxymitorubrinol (**4**); (+)-mitorubrinol (**5**); sporothriolide (**6**); dihydroisosporothric acid (**7**); cohaerin E (**8**); 8-methoxy naphthol (**9**); 1,8-naphthol (**10**); hypoxylone (**11**).

Another species that was retained in *Hypoxylon*, even though the DNA sequences of the only available strain formed an aberrant clade in the phylogeny by Wendt et al. (2018) is *H. papillatum* Ellis & Everh. This species is characterized by effused-pulvinate stromata featuring long tubular perithecia. Therefore, its stromata somewhat resemble those of *Pyrenopolyporus* and certain *Daldinia* species such as *D. placentiformis* that do not have internal concentric zones. Ju and Rogers (1996) have studied the type material and concluded that the syntypes they studied from BPI and NY (i.e., the specimens listed in the protologue by Ellis and Everhart (see Smith 1893) did not all correspond to the same taxon. They identified some of the specimens as *Hypoxylon placentiforme* (now: *Daldinia placentiformis*), which was confirmed by Stadler et al. (2014) in the *Daldinia* world monograph, and selected a lectotype from Ohio (Commons No. 2160) which showed a characteristic morphology and could easily be distinguished from the former taxon. They also listed several other specimens from North America and Trinidad that showed the same characteristics.

Rogers (1985) cultured this fungus and provided a detailed description of its nodulisporium-like anamorph and culture. The corresponding specimen was collected by him in West Virginia, USA, and could have served as epitype. The culture is deposited in ATCC and showed the typical characteristics of *H. papillatum* sensu Rogers (1985) and was included in the phylogeny by Wendt et al. (2018) as a representative of this taxon. However, it showed an aberrant phylogenetic position in a clade that appeared basal to the others in which the DNA sequences of *Hypoxylon* species were located. We have come across a very similar fungus that was collected in Central Africa and have studied it, along with several extant type and authentic specimens for comparison. The results of this study, which also relies on state-of-the art metabolomics, are reported herein.

## Materials and methods

### Sample sources

All scientific names of fungi are given without authorities or publication details, according to Index Fungorum (http://www.indexfungorum.org). Type and reference specimens were provided by Washington State University herbarium (**WSP**), U.S. National Fungus Collections (**BPI**) and the New York Botanical Garden (**NY**), USA. Fungal cultures were provided from the Belgian Coordinated Collections of Microorganisms (**MUCL**), Belgium and the Westerdijk Fungal Biodiversity Institute (**CBS**), The Netherlands.

### Morphological characterization

The microscopic characteristics of the teleomorph were carried out as described by Pourmoghaddam et al. (2020). To observe the macro-morphology of the cultures, the strains were grown on Difco Oatmeal Agar (**OA**), 2% Malt Extract Agar (**MEA**) and Yeast Malt agar (**YM** agar; malt extract 10 g/L, yeast extract 4 g/L, D-glucose 4 g/L, agar 20 g/L, pH 6.3 before autoclaving) and the cultures checked at 15 days after inoculation. Pigment colors were determined following the color-codes by Rayner (1970).

## DNA extraction, PCR and sequencing

The DNA was extracted from pure cultures grown on plates with YM agar. Small amounts of mycelia were harvested after five days of growth and transferred to a 1.5 ml homogenization tube filled with six to eight Precellys Ceramic beads (1.4 mm, Bertin Technologies, Montigny-le-Bretonneux, France).

DNA extraction was performed using the commercially available Fungal gDNA Miniprep Kit EZ-10 spin column (NBS Biologicals, Cambridgeshire, UK) following the manufacturer's instructions. The *tub2* (partial β-tubulin) gene region was amplified using the primers T1 and T22 (O'Donnell and Cigelnik 1997); ITS (nuc rDNA internal transcribed spacer) region using the primers ITS4 and ITS5 (White et al. 1990); LSU (Large subunit nuc 28S rDNA) using LR0R and LR7 (Vilgalys and Hester 1990) and *rpb2* (partial second largest subunit of the DNA-directed RNA polymerase II) using fRPB2-5F and fRPB2-7cR (Liu et al. 1999).

PCR reactions were performed by mixing template gDNA (2–3 µL), 12.5 µL JumpStart Taq Ready Mix (Sigma Aldrich, Deisenhofen, Germany), 0.5 µL of both forward and reverse primers (10 mM) and 8.5 to 9.5 µl of sterile filtered and sterilized water to a final volume of 25 µL. Amplification was achieved using a Mastercycler nexus Gradient (Eppendorf, Hamburg, Germany). Thermocycling for ITS commenced with an initial denaturation at 94 °C for 5 min followed by 34 cycles of denaturation (30 s at 94 °C), annealing (30 s at 52 °C), and elongation (1 min at 72 °C). The program concluded with a 10 min lasting elongation at 72 °C and reaction tubes were stored at 4 °C until further use. In the case of the other loci, the following steps were modified: LSU denaturation (1 min at 94 °C), annealing (1 min at 52 °C), and elongation (2 min at 72 °C); For *tub2* the cycle repetitions were raised to 38, annealing (30 s at 47 °C) and elongation (2 min 30 s at 72 °C); for *rpb2,* the cycle repetitions were raised to 38, annealing (1 min at 54 °C) and elongation (1 min 30 s at 72 °C).

## Molecular phylogenetic analyses

Sequences were analyzed and processed in Geneious 7.1.9 (Kearse et al. 2012). The generated sequence data were complemented by available sequence data from GenBank and the data sets for each genetic marker were aligned using MAFFT online (http://mafft.cbrc.jp/alignment/server/, Katoh et al. 2019), and manually curated in MEGA 11 (Tamura et al. 2021). A maximum-likelihood phylogenetic tree was constructed using IQ-TREE v. 2.1.3 [-b 1000 -abayes -m MFP -nt AUTO] (Minh et al. 2020), The selection of the appropriate nucleotide exchange model was selected by ModelFinder (Chernomor et al. 2016; Kalyaanamoorthy et al. 2017) based on Bayesian inference criterion. Branch support was calculated with non-parametric bootstrap (Felsenstein 1985 and approximate Bayes test (Anisimova et al. 2011). The total 1000 bootstrap replicates were mapped onto the ML tree with the best (highest) ML score. Single locus trees were calculated following the identical methodology and checked for congruence with the multigene phylogenetic tree.

A second phylogenetic inference was carried out following a Bayesian approach using MrBayes 3.2.7a (Ronquist et al. 2012) with algorithm options set to the ones

reported by Matio Kemkuignou et al. (2022). The data matrix was subjected to PartitionFinder2 (Lanfear et al. 2016) as implemented in the program package phylosuite v. 1.2.2 (Zhang et al. 2020) with settings set to an un-linked determination of the best-fitting nucleotide substitution models following Bayesian information criterion (BIC) for the different partitions, restricted to the ones available in MrBayes. Posterior probabilities (PP) above 95% were regarded as significant. To determine the congruence of the topologies of ML and Bayes, an approximate unbiased (AU) topology test was carried out in IQ-TREE [iqtree -s example.phy -z example.treels -n 0 -zb 10000 -zw -au](Shimodaira 2022). All sequences used for the pyhlogeny are listed in Table 1.

## UHPLC profiling and dereplication

The secondary metabolites were extracted using a small piece of the stromata (approx. 1 $mm^3$). Each piece was placed in 1.5 ml reaction tubes, covered with 1000 µl of methanol and placed for 30 min at 40 °C in an ultrasonic bath. The tubes were centrifuged at 14 000 rpm for 10 min. The methanol extract was separated from the remaining stromata, which was extracted again under the same procedure. Finally, both organic phases were combined and dried under nitrogen. Each sample was analyzed at a concentration of 450 µg/mL on an ultrahigh performance liquid chromatography system (Dionex Ultimate3000RS, Thermo Scientific, Dreieich, Germany), using a C18 column (Kinetex 1.7 µm, 2.1 × 150 mm, 100 Å; Phenomenex, Aschaffenburg, Germany) with a sample injection volume of 2 µL. The mobile phase consisted of A ($H_2O$ + 0.1% formic acid) and B (ACN + 0.1% formic acid) with a constant flow rate of 0.3 mL/min. The gradient began with 1% B for 0.5 min, increasing to 5% B in 1 min, then to 100% B in 19 min and holding at 100% B for 5 min. The temperature of the column was kept at 40 °C and UV-Vis data were recorded with a DAD at 190–600 nm.

MS spectra were collected using a trapped ion mobility quadrupole time-of-flight mass spectrometer (timsTOF Pro, Bruker Daltonics, Bremen, Germany) with the following parameters: tims ramp time 100 ms, spectra rate 9.52 Hz, PASEF on, cycle time 320 ms, MS/MS scans 2, scan range (*m/z*, 100–1800 Da; $1/k_0$, 0.55–2.0 V·s/$cm^2$). For the stromatal extracts and the standards ESI mass spectra were acquired in positive ion mode. Raw data were pre-processed with MetaboScape 2022 (Bruker Daltonics, Bremen, Germany) in the retention time range of 0.5 to 25 min. The obtained features were dereplicated against our in-house database comprising MS/MS spectra of standards from characteristic secondary metabolites of hypoxylaceous species (e.g. azaphilones, asterriquinones, binaphthalenes, cytochalasins, macrolides and sesquiterpenoids) in MetaboScape. A molecular network was created with the Feature-Based Molecular Networking (FBMN) (Nothias et al. 2020) and the Spec2Vec (Huber et al. 2021) workflows on the GNPS platform (Wang et al. 2016) using the pre-processed feature table from MetaboScape. Fragmentation ions resulting from the MS/MS spectra of cohaerin E, cohaerin H, and minutellin A were assigned using CFM-ID 4.0 web server (Wang et al. 2021) and validated with the SmartFormula 3D tool from MetaboScape. The datasets generated/analyzed for this study are included in Suppl. material 1.

**Table 1.** Strains used in the phylogenetic analyses, including the strain IDs, GenBank accession numbers, and the references where the sequence data have been originally generated. Type specimens are labeled with T (holotype), IT (isotype), PT (paratype) and ET (epitype).

| Species | Strain number | GenBank Accession Number | | | | Origin | References |
|---|---|---|---|---|---|---|---|
| | | ITS | LSU | *rpb2* | *tub2* | | |
| *Annulohypoxylon annulatum* | CBS 140775 | KY610418 | KY610418 | KY624263 | KX376353 | USA (ET) | Kuhnert et al. (2017a; *tub2*), Wendt et al. (2018: ITS, LSU, *rpb2*) |
| *Annulohypoxylon michelianum* | CBS 119993 | KX376320 | KY610423 | KY624234 | KX271239 | Spain | Kuhnert et al. (2014a; ITS, *tub2*), Wendt et al. (2018; LSU, *rpb2*) |
| *Annulohypoxylon truncatum* | CBS 140778 | KY610419 | KY610419 | KY624277 | KX376352 | USA (ET) | Kuhnert et al. (2017a; *tub2*), Wendt et al. (2018; ITS, LSU, *rpb2*) |
| *Daldinia bambusicola* | CBS 122872 | KY610385 | KY610431 | KY624241 | AY951688 | Thailand (T) | Hsieh et al. (2005; *tub2*), Wendt et al. (2018; ITS, LSU, *rpb2*) |
| *Daldinia childiae* | CBS 122881 | KU683757 | MH874773 | KU684290 | KU684129 | France (T) | U'Ren et al. (2016; ITS, *tub2*, *rpb2*), Vu et al. (2019; LSU) |
| *Daldinia concentrica* | CBS 113277 | AY616683 | KY610434 | KY624243 | KC977274 | Germany | Triebel et al. (2005; ITS), Kuhnert et al. (2014a; *tub2*), Wendt et al. (2018; LSU, *rpb2*) |
| *Daldinia dennisii* | CBS 114741 | JX658477 | KY610435 | KY624244 | KC977262 | Australia (T) | Stadler et al. (2014; ITS), Kuhnert et al. (2014a; *tub2*), Wendt et al. (2018; LSU, *rpb2*) |
| *Daldinia eschscholtzii* | MUCL 45435 | JX658484 | KY610437 | KY624246 | KC977266 | Benin | Stadler et al. (2014a; ITS), Kuhnert et al. (2014a; *tub2*), Wendt et al. (2018; LSU, *rpb2*) |
| *Daldinia petriniae* | MUCL 49214 | AM749937 | KY610439 | KY624248 | KC977261 | Austria (ET) | Bitzer et al. (2008; ITS), Kuhnert et al. (2014a; *tub2*), Wendt et al. (2018; LSU, *rpb2*) |
| *Daldinia placentiformis* | MUCL 47603 | AM749921 | KY610440 | KY624249 | KC977278 | Mexico | Stadler et al. (2014a; ITS), Kuhnert et al. (2014a; *tub2*), Wendt et al. (2018; LSU, *rpb2*) |
| *Daldinia vernicosa* | CBS 119316 | KY610395 | KY610442 | KY624252 | KC977260 | Germany (ET) | Kuhnert et al. (2014a; *tub2*), Wendt et al. (2018; ITS, LSU, *rpb2*) |
| *Durotheca rogersii* | YMJ 92031201 | EF026127 | | JX507794 | EF025612 | Taiwan | Ju et al. (2007) as *Theissenia* |
| *Durotheca comedens* | YMJ 90071615 | EF026128 | | JX507793 | EF025613 | Taiwan (T) | Ju et al. (2003) as *Theissenia* |
| *Durotheca crateriformis* | GMBC0205 | MH645426 | MH645425 | MH645427 | MH049441 | China (T) | de Long et al. (2019) |
| *Durotheca guizhouensis* | GMBC0065 | MH645423 | MH645421 | MH645422 | MH049439 | China (T) | de Long et al. (2019) |
| *Durotheca rogersii* | GMBC0204 | MH645433 | MH645434 | MH645435 | MH049449 | China | de Long et al. (2019) |
| *Graphostroma platystomum* | CBS 270.87 | JX658535 | DQ836906 | KY624296 | HG934108 | France (T) | Zhang et al. (2006; LSU), Stadler et al. (2014; ITS), Koukol et al. (2015; *tub2*), Wendt et al. (2018; *rpb2*) |
| *Hypomontagnella barbarensis* | STMA 14081 | MK131720 | MK131718 | MK135891 | MK135893 | Argentina (T) | Lambert et al. (2019) |
| *Hypomontagnella monticulosa* | MUCL 54604 | KY610404 | KY610487 | KY624305 | KX271273 | French Guiana | Wendt et al. (2018) |
| *Hypomontagnella submonticulosa* | CBS 115280 | KC968923 | KY610457 | KY624226 | KC977267 | France | Kuhnert et al. (2014a; ITS, *tub2*), Wendt et al. (2018; LSU, *rpb2*) |
| *Hypoxylon addis* | MUCL 52797 | KC968931 | ON954141 | OP251037 | KC977287 | Ethiopia (T) | Kuhnert et al. (2014a; ITS, *tub2*), This study |
| *Hypoxylon aveirense* | MUM 19.40 | MN053021 | ON954142 | OP251028 | MN066636 | Portugal (T) | Vicente et al. (2021; ITS, *tub2*), This study |
| *Hypoxylon baruense* | UCH9545 | MN056428 | ON954143 | | MK908142 | Panama (T) | Cedeño–Sanchez et al. (2020; ITS, *tub2*); This study |
| *Hypoxylon canariense* | MUCL 47224 | ON792787 | ON954140 | OP251029 | ON813073 | Spain, Canary Islands (PT) | This study. (Species described by Stadler et al. 2008) |
| *Hypoxylon carneum* | MUCL 54177 | KY610400 | KY610480 | KY624297 | KX271270 | France | Wendt et al. (2018) |
| *Hypoxylon cercidicola* | CBS 119009 | KC968908 | KY610444 | KY624254 | KC977263 | France | Kuhnert et al. (2014a; ITS, *tub2*), Wendt et al. (2018; LSU, *rpb2*) |
| *Hypoxylon chionostomum* | STMA 14060 | KU604563 | ON954144 | OP251030 | ON813072 | Argentina | Sir et al. (2016; ITS); This study |

| Species | Strain number | GenBank Accession Number | | | | Origin | References |
|---|---|---|---|---|---|---|---|
| | | ITS | LSU | *rpb2* | *tub2* | | |
| *Hypoxylon chrysalidosporum* | FCATAS2710 | OL467294 | OL615106 | OL584222 | OL584229 | China (T) | Ma et al. (2022) |
| *Hypoxylon crocopeplum* | CBS 119004 | KC968907 | KY610445 | KY624255 | KC977268 | France | Kuhnert et al. (2014a; ITS, *tub2*), Wendt et al. (2018; LSU, *rpb2*) |
| *Hypoxylon cyclobalanopsidis* | FCATAS2714 | OL467298 | OL615108 | OL584225 | OL584232 | China (T) | Ma et al. (2022) |
| *Hypoxylon erythrostroma* | MUCL 53759 | KC968910 | ON954154 | OP251031 | KC977296 | Martinique | Kuhnert et al. (2014a; ITS2, TUB), This study |
| *Hypoxylon eurasiaticum* | MUCL 57720 | MW367851 | | MW373852 | MW373861 | Iran (T) | Lambert et al. (2021) |
| *Hypoxylon fendleri* | MUCL 54792 | KF234421 | KY610481 | KY624298 | KF300547 | French Guiana | Kuhnert et al. (2014a; ITS, *tub2*), Wendt et al. (2018; LSU, *rpb2*) |
| *Hypoxylon ferrugineum* | CBS 141259 | KX090079 | | | KX090080 | Austria | Friebes and Wendelin (2016) |
| *Hypoxylon fragiforme* | MUCL 51264 | KC477229 | KM186295 | MK887342 | KX271282 | Germany (ET) | Stadler et al. (2013; ITS), Daranagama et al. (2015; LSU, *rpb2*), Wendt et al. (2018; *tub2*) |
| *Hypoxylon fuscoides* | MUCL 52670 | ON792789 | ON954145 | OP251038 | ON813076 | France (T) | This study. (Species described by Fournier et al. 2010a) |
| *Hypoxylon fuscum* | CBS 113049 | KY610401 | KY610482 | KY624299 | KX271271 | Germany (ET) | Wendt et al. (2018) |
| *Hypoxylon gibriacense* | MUCL 52698 | KC968930 | ON954146 | OP251026 | ON813074 | France (T) | Kuhnert et al. (2014a; ITS). This study |
| *Hypoxylon griseobrunneum* | CBS 331.73 | KY610402 | KY610483 | KY624300 | KC977303 | India (T) | Kuhnert et al. (2014a; *tub2*), Wendt et al. (2018; ITS, LSU, *rpb2*) |
| *Hypoxylon guilanense* | MUCL 57726 | MT214997 | MT214992 | MT212235 | MT212239 | Iran (T) | Pourmoghaddam et al. (2020) |
| *Hypoxylon haematostroma* | MUCL 53301 | KC968911 | KY610484 | KY624301 | KC977291 | Martinique (ET) | Wendt et al. (2018; LSU, *rpb2*), Kuhnert et al. (2014a; ITS, *tub2*), |
| *Hypoxylon hainanense* | FCATAS2712 | OL467296 | OL616132 | OL584224 | OL584231 | China (T) | Ma et al. (2022) |
| *Hypoxylon hinnuleum* | ATCC 36255, MUCL 3621 | MK287537 | MK287549 | MK287562 | MK287575 | USA (T) | Sir et al. (2019) |
| *Hypoxylon howeanum* | MUCL 47599 | AM749928 | KY610448 | KY624258 | KC977277 | Germany | Bitzer et al. (2008; ITS), Kuhnert et al. (2014a; *tub2*), Wendt et al. (2018; LSU, *rpb2*) |
| *Hypoxylon hypomiltum* | MUCL 51845 | KY610403 | KY610449 | KY624302 | KX271249 | Guadeloupe | Wendt et al. (2018) |
| *Hypoxylon invadens* | MUCL 51475 | MT809133 | MT809132 | MT813037 | MT813038 | France (T) | Becker et al. (2020) |
| *Hypoxylon investiens* | CBS 118183 | KC968925 | KY610450 | KY624259 | KC977270 | Malaysia | Kuhnert et al. (2014a; ITS, *tub2*), Wendt et al. (2018; LSU, *rpb2*) |
| *Hypoxylon isabellinum* | MUCL 53308 | KC968935 | ON954155 | OP251032 | KC977295 | Martinique (T) | Kuhnert et al. (2014a; ITS, *tub2*), This study |
| *Hypoxylon laschii* | MUCL 52796 | JX658525 | ON954147 | OP251027 | ON813075 | France | Stadler et al. (2014; ITS), This study |
| *Hypoxylon lateripigmentum* | MUCL 53304 | KC968933 | KY610486 | KY624304 | KC977290 | Martinique (T) | Kuhnert et al. (2014a; ITS, *tub2*), Wendt et al. (2018; LSU, *rpb2*) |
| *Hypoxylon lechatii* | MUCL 54609 | KF923407 | ON954148 | OP251033 | KF923405 | French Guiana | Kuhnert et al. (2014b; ITS, *tub2*), This study |
| *Hypoxylon lenormandii* | CBS 119003 | KC968943 | KY610452 | KY624261 | KC977273 | Ecuador | Kuhnert et al. (2014a; ITS, *tub2*), Wendt et al. (2018; LSU, *rpb2*) |
| *Hypoxylon lienhwacheense* | MFLUCC 14-1231 | KU604558 | MK287550 | MK287563 | KU159522 | Thailand | Sir et al. (2016; ITS, *tub2*), Sir et al. (2019; LSU, *rpb2*) |
| *Hypoxylon lividipigmentum* | STMA14045 | ON792788 | ON954149 | | ON813077 | Argentina | This study |
| *Hypoxylon lividipigmentum* | BCRC 34077 | JN979433 | | | AY951735 | Mexico (IT) | Hsieh et al. (2005) |
| *Hypoxylon macrocarpum* | CBS119012 | ON792785 | ON954151 | OP251034 | ON813071 | Germany | This study |
| *Hypoxylon munkii* | MUCL 53315 | KC968912 | ON954153 | OP251035 | KC977294 | Martinique | Kuhnert et al. (2014a; ITS, *tub2*), This study |
| *Hypoxylon musceum* | MUCL 53765 | KC968926 | KY610488 | KY624306 | KC977280 | Guadeloupe | Kuhnert et al. (2014a; ITS, *tub2*), Wendt et al. (2018; LSU, *rpb2*) |
| *Hypoxylon ochraceum* | MUCL 54625 | KC968937 | | KY624271 | KC977300 | Martinique (ET) | Kuhnert et al. (2014a; ITS, *tub2*), Wendt et al. (2018; *rpb2*) |

| Species | Strain number | GenBank Accession Number | | | | Origin | References |
|---|---|---|---|---|---|---|---|
| | | ITS | LSU | *rpb2* | *tub2* | | |
| *Hypoxylon olivaceopigmentum* | DSM 107924 | MK287530 | MK287542 | MK287555 | MK287568 | USA (T) | Sir et al. (2019) |
| *Hypoxylon perforatum* | CBS115281 | KY610391 | KY610455 | KY624224 | KX271250 | France | Wendt et al. (2018) |
| *Hypoxylon petriniae* | CBS 114746 | KY610405 | KY610491 | KY624279 | KX271274 | France (T) | Wendt et al. (2018) |
| *Hypoxylon pilgerianum* | STMA 13455 | KY610412 | KY610412 | KY624308 | KY624315 | Martinique | Wendt et al. (2018) |
| *Hypoxylon porphyreum* | CBS 119022 | KC968921 | KY610456 | KY624225 | KC977264 | France | Kuhnert et al. (2014a; ITS, *tub2*), Wendt et al. (2018; LSU, *rpb2*) |
| *Hypoxylon pseudofuscum* | DSM112038 | MW367857 | MW367848 | MW373858 | MW373867 | Germany (T) | Lambert et al. (2021) |
| *Hypoxylon pulicicidum* | CBS 122622 | JX183075 | KY610492 | KY624280 | JX183072 | Martinique (T) | Bills et al. (2012; ITS, *tub2*), Wendt et al. (2018; LSU, *rpb2*) |
| *Hypoxylon rickii* | MUCL 53309 | KC968932 | KY610416 | KY624281 | KC977288 | Martinique (ET) | Kuhnert et al. (2014a; ITS, *tub2*), Wendt et al. (2018; LSU, *rpb2*) |
| *Hypoxylon rubiginosum* | MUCL 52887 | KC477232 | KY610469 | KY624266 | KY624311 | Germany (ET) | Stadler et al. (2013; ITS), Wendt et al. (2018; *tub2*, LSU, *rpb2*) |
| *Hypoxylon samuelsii* | MUCL 51843 | KC968916 | KY610466 | KY624269 | KC977286 | Guadeloupe (ET) | Kuhnert et al. (2014a; ITS, *tub2*), Wendt et al. (2018; LSU, *rpb2*) |
| *Hypoxylon sporistriatatunicum* | | MN056426 | ON954150 | OP251036 | MK908140 | Panama (T) | Cedeño-Sanchez et al. (2020; ITS, *tub2*); This study |
| *Hypoxylon subticinense* | MUCL 53752 | KC968913 | ON954152 | | KC977297 | French Guiana | Kuhnert et al. (2014a; ITS, *tub2*), This study |
| *Hypoxylon texense* | DSM 107933 | MK287536 | MK287548 | MK287561 | MK287574 | USA (T) | Sir et al. (2019) |
| *Hypoxylon ticinense* | CBS 115271 | JQ009317 | KY610471 | KY624272 | AY951757 | France | Hsieh et al. (2005; ITS, *tub2*), Wendt et al. (2018; LSU, *rpb2*) |
| *Hypoxylon trugodes* | MUCL 54794 | KF234422 | KY610493 | KY624282 | KF300548 | Sri Lanka (ET) | Kuhnert et al. (2014a; ITS, *tub2*), Wendt et al. (2018; LSU, *rpb2*) |
| *Hypoxylon vogesiacum* | CBS 115273 | KC968920 | KY610417 | KY624283 | KX271275 | France | Kuhnert et al. (2014a; ITS), Kuhnert et al. (2017a; *tub2*), Wendt et al. (2018; LSU, *rpb2*) |
| *Hypoxylon wuzhishanense* | FCATAS2708 | OL467292 | OL615104 | OL584220 | OL584227 | China (T) | Ma et al. (2022) |
| *Jackrogersella cohaerens* | CBS 119126 | KY610396 | KY610497 | KY624270 | KY624314 | Germany | Wendt et al. (2018) |
| *Jackrogersella multiformis* | CBS 119016 | KC477234 | KY610473 | KY624290 | KX271262 | Germany (ET) | Kuhnert et al. (2014a ; ITS), Kuhnert et al. (2017a; *tub2*), Wendt et al. (2018; LSU, *rpb2*) |
| *Natonodosa speciosa* | CLM-RV86 | MF380435 | MF380435 | MH745150 | | Mexico (T) | Heredia et al. (2020) |
| *Parahypoxylon papillatum* comb. nov. | ATCC 58729 | KC968919 | KY610454 | KY624223 | KC977258 | USA (T) | Kuhnert et al. (2014a; ITS, *tub2*), Wendt et al. (2018; LSU, *rpb2*) |
| *Parahypoxylon ruwenzoriense* sp. nov. | MUCL51392 | ON792786 | ON954156 | OP251039 | ON813078 | D. R. Congo (T) | This study |
| *Pyrenopolyporus hunteri* | MUCL 52673 | KY610421 | KY610472 | KY624309 | KU159530 | Ivory Coast (ET) | Kuhnert et al. (2017a; *tub2*), Wendt et al. (2018; ITS, LSU, *rpb2*) |
| *Pyrenopolyporus laminosus* | MUCL 53305 | KC968934 | KY610485 | KY624303 | KC977292 | Martinique (T) | Kuhnert et al. (2014a; ITS, *tub2*), Wendt et al. (2018; LSU, *rpb2*) |
| *Pyrenopolyporus nicaraguense* | CBS 117739 | AM749922 | KY610489 | KY624307 | KC977272 | Burkina_Faso | Bitzer et al. (2008; ITS), Kuhnert et al. (2014a; *tub2*), Wendt et al. (2018; LSU, *rpb2*) |
| *Rhopalostroma angolense* | CBS 126414 | KY610420 | KY610459 | KY624228 | KX271277 | Ivory Coast | Wendt et al. (2018) |
| *Rostrohypoxylon terebratum* | CBS 119137 | DQ631943 | DQ840069 | DQ631954 | DQ840097 | Thailand (T) | Tang et al. (2007), Fournier et al. (2010b) |
| *Ruwenzoria pseudoannulata* | MUCL 51394 | KY610406 | KY610494 | KY624286 | KX271278 | D. R. Congo (T) | Wendt et al. (2018) |
| *Thamnomyces dendroidea* | CBS 123578 | FN428831 | KY610467 | KY624232 | KY624313 | French Guiana (T) | Stadler et al. (2010; ITS), Wendt et al. (2018; *tub2*, LSU, *rpb2*) |
| *Xylaria arbuscula* | CBS 126415 | KY610394 | KY610463 | KY624287 | KX271257 | Germany | Fournier et al. (2011; ITS), Wendt et al. (2018; *tub2*, LSU, *rpb2*) |
| *Xylaria hypoxylon* | CBS 122620 | KY610407 | KY610495 | KY624231 | KX271279 | Sweden (ET) | Wendt et al. (2018) |

# Results

## Phylogenetic analyses

The final data matrix for the molecular phylogenetic analysis (Fig. 2) comprised 345 sequences (44 generated in this study, and complemented by sequences available from GenBank, NCBI) derived from 89 strains and four loci, namely ITS, LSU, *rpb2* and *tub2*. The final MAFFT alignments consisted of 4018 nucleotides for the ITS alignment, 3642 for the LSU alignment, 2238 for the *tub2* alignment and 4023 positions for the *rpb2* alignment. The alignment of each locus is available in the Suppl. material 1: table S3–S6. Sequences of representatives for each molecularly well-established genus of the Hypoxylaceae were included: *Annulohypoxylon* (3 strains), *Daldinia* (8 strains), *Durotheca* (5 strains), *Hypomontagnella* (3 strains), *Hypoxylon* (58 strains), *Jackrogersella* (2 strains), *Natonodosa* (1 strain), *Pyrenopolyporus* (3 strains), as well as *Rhopalostroma*, *Rostrohypoxylon*, *Ruwenzoria*, and *Thamnomyces* (1 strain each). Three members of Xylariaceae and Graphostromataceae (*Xylaria hypoxylon*, *X. arbuscula* and *Graphostroma platystomum*) served as outgroup.

The inference of phylogenetic relationship using a Maximum-Likelihood and Bayesian approach yielded two different, discongruent topologies. An approximate unbiased (AU) topology test implemented in IQTree indicated that the tree resulting from Bayesian inference received a significantly ($p < 0.05$) lower maximum likelihood score, suggesting its rejection. Hence, we included support values of the approximate Bayes test implemented in IQTree to access posterior probability support values of the inferred phylogenetic tree. The combined rooted phylogenetic tree showed a clade consisting of the core members of the Hypoxylaceae, such as *Hypoxylon*, *Daldinia*, *Pyrenopolyporus*, *Hypomontagnella*, *Jackrogersella*, *Rostrohypoxylon*, *Thamnomyces* and *Ruwenzoria* with medium BS and high PP support (1/90), which was placed in a sister position to a clade consisting of members of *Parahypoxylon* gen. nov., and *Durotheca* (Hypoxylaceae) at the base of the tree with strong support (1/100). The genus *Hypoxylon* could be confirmed as paraphyletic, as has been described already by Wendt et al. (2018), Lambert et al. (2019), and Becker et al. (2020). The sequences assigned to *Parahypoxylon ruwenzoriense* formed a highly supported (1/100) cluster with the sequences derived from *Parahypoxylon papillatum*. The topology of *Durotheca* and the newly described genus *Parahypoxylon* as a basal lineage in the Hypoxylaceae are further reflected upon in the taxonomic part of this study.

## Taxonomy

### Lecto- and epitypification

### *Hypomontagnella monticulosa* (Mont.) Sir, L. Wendt & C. Lamb.

**Type.** French Guiana, Cayenne, Leprieur, C. 1176, dead wood (PC, holotype; FH, isotype of *H. monticulosum*).

**Epitype (designated here).** France. French Guyana, Sinnamary, Paracou, Amazonian rain forest, bark of unknown tree, June 2012, leg J. Fournier (LIP, ex-epitype

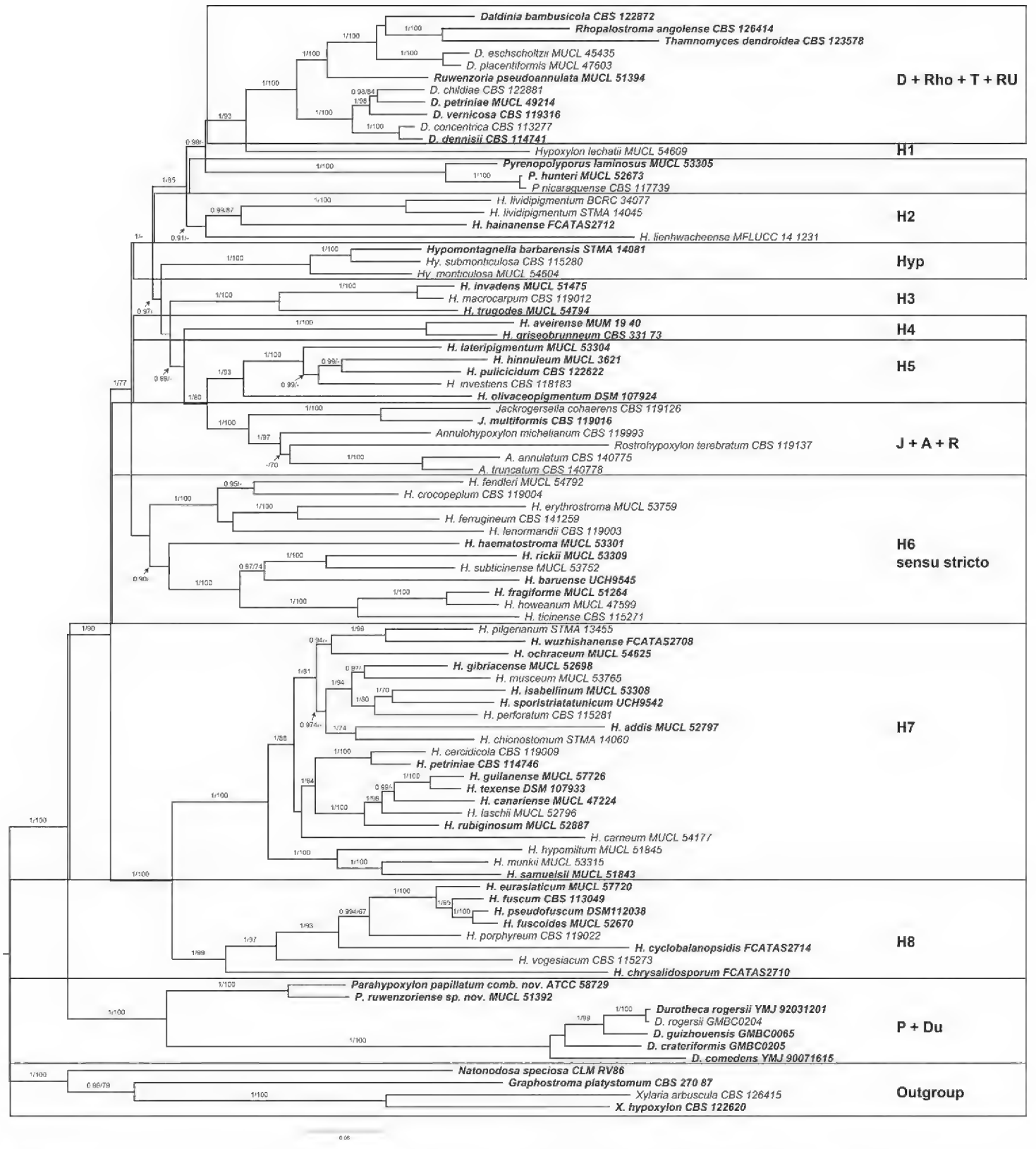


**Figure 2.** Inferred molecular phylogenetic maximum Likelihood (lLn = -122825.7921) tree of selected Hypoxylaceae, Graphostromataceae and Xylariaceae sequences. The analysis was calculated by using IQ-Tree with posterior probability support calculated from Bayesian inference methodology and support values generated from 1000 bootstrap replicates using a multigene alignment (ITS, LSU, *tub*2 and *rpb*2). The tree was rooted with *Xylaria hypoxylon* CBS 122620, *X. arbuscula* CBS 126415 (Xylariaceae) and *Graphostroma platystomum* CBS 27087 (Graphostromataceae). Type material is highlighted in **bold** letters. Bayesian posterior probability scores ≥ 0.95 / Bootstrap support values ≥ 70 are indicated along branches.

culture MUCL 54604). GenBank acc. nos for DNA sequences: KY610404 and KJ810556 (ITS), KY610487 (LSU), KY624305 (*rpb*2), KX271273 (*tub2*); MT889334 (sporothriolide gene cluster published by Tian et al. 2020).

MBT no: 10010042.

**Notes.** The strain designated here as epitype was used by Lambert et al. (2019) and the subsequent publications on genome analysis (Stadler et al. 2020; Tian et al. 2020; Kuhnert et al. 2021; Wibberg et al. 2021). The specimen and culture are perfectly suitable, because it was collected from the same geographic area as the holotype.

***Parahypoxylon*** **M. Cedeño-Sanchez, E. Charria-Girón & M. Stadler, gen. nov.**
MycoBank No: 845463

**Etymology.** Refers to the morphological similarity to *Hypoxylon*, from which the genus is phylogenetically distinct.

**Diagnosis.** Differs from the genus *Durotheca* by the presence of greenish KOH-extractable pigments and by having an amyloid ascal apical apparatus. Differs from the genus *Hypoxylon* by containing yet unknown cohaerin-type azaphilones and by its basal position in the molecular phylogenetic inference using am ITS, LSU, *rpb2* and *tub2* matrix.

***Parahypoxylon papillatum*** **(Ellis & Everh) M. Cedeño-Sanchez, E. Charria-Girón & M. Stadler, comb. nov.**
MycoBank No: 845462
Figs 3, 4

*Hypoxylon papillatum* Ellis & Everh. in Smith, Bull. Lab. Nat. Hist. Iowa State Univ. 2: 408 (1893). Syn.

**Lectotype.** USA. Ohio, Delaware, 21 Jul 1893, A. Commons 2160, rotten wood of *Carya* (NY [2 pks.], selected by Ju and Rogers (1996).

**Epitype.** USA. West Virginia, Mason Co., Bruce's Chapel, 18 Aug 1983, wood of *Acer*, J.D. Rogers (WSP 7557; ex-epitype culture ATCC 58729).

MBT no: 10011515.

**Teleomorph.** Stromata superficial, effused-pulvinate to plane, with inconspicuous to conspicuous perithecial mounds, up to 12.5 cm long × up to 4 cm broad × 1.8–4.0 mm thick; surface Honey (64) to Isabelline (65), Isabelline (65) to Gray Olivaceous (107), or Isabelline (65) to Olivaceous (48); blackish granules immediately beneath surface and between perithecia, with KOH-extractable pigments Isabelline (65); the tissue below the perithecial layer conspicuous, black, 1.0–2.5 mm thick. Perithecia long-tubular, 0.3–0.4 mm diam × 0.8–1.5 mm high. Ostioles umbilicate. Asci with amyloid, discoid apical apparatus, 1–2 µm high × 3.5 µm wide, stipe up 137–180 µm long × 8–10 µm broad, the spore-bearing parts 93–110 µm long, the stipes 30–80 µm long. Ascospores brown to dark brown, unicellular, ellipsoid, nearly equilateral, with broadly to narrowly rounded ends, 12.0–18.5 × 6.5–9.0 µm, with straight germ slit spore-length; perispore indehiscent in 10% KOH; epispore smooth.

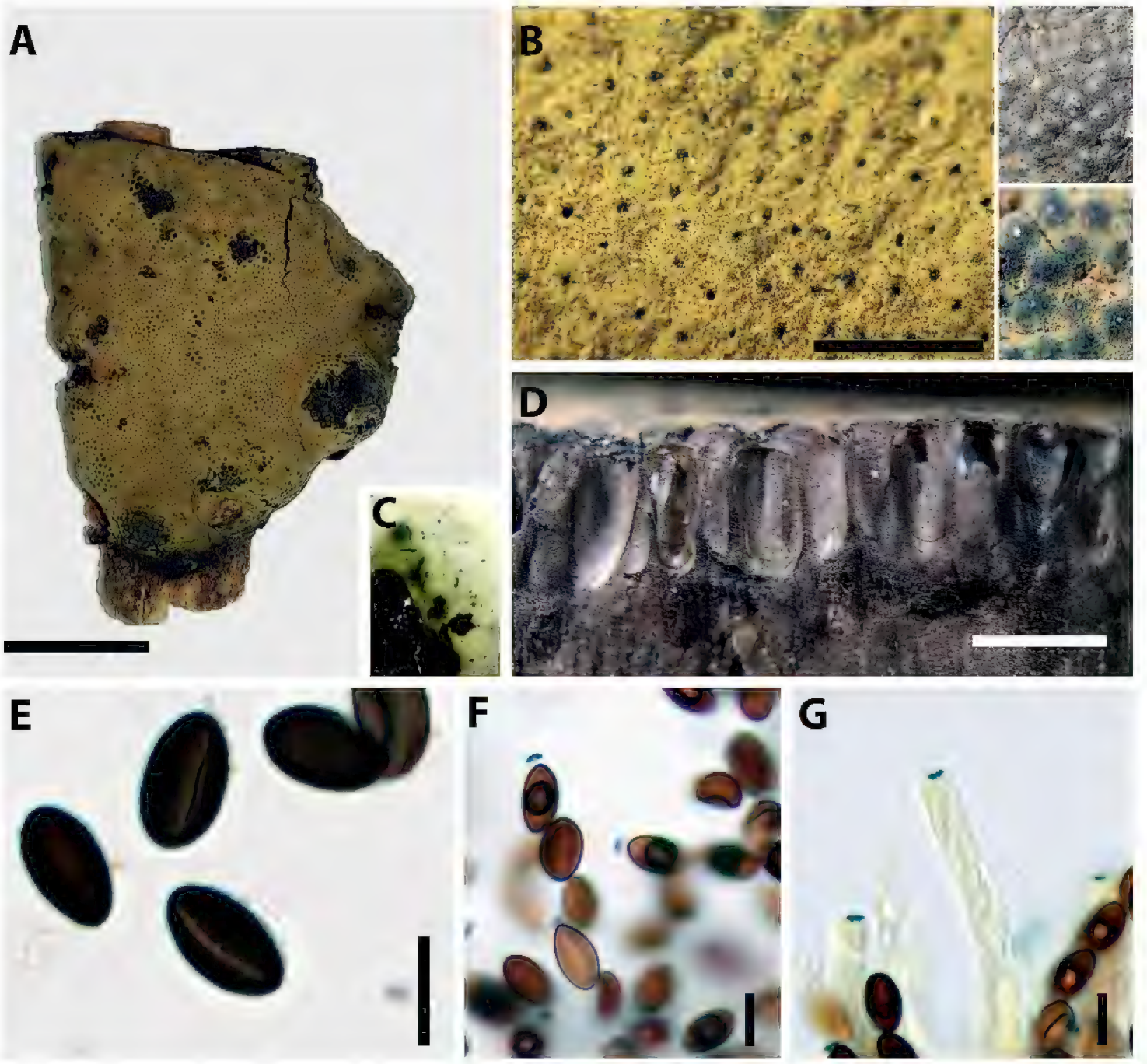


**Figure 3.** *Parahypoxylon papillatum* comb. nov. **A** stroma **B** ostioles **C** KOH extractable stromatal pigments **D** perithecia (cross section) **E** ascospores with straight germ slits **F** amyloid apical apparatus in a mature ascus treated with Melzer's reagent **G** amyloid apical apparatus in an immature ascus treated with Melzer's reagent. Scale bars: 1 cm (**A**); 10 µm (**E–F**); 10 µm (**G**).

**Cultures and anamorph.** Colonies on MEA, OA, and YM covering a 9 cm Petri plate in 2 weeks, with white, flat, mycelium, margins filamentous. Reverse at first white, becoming yellowish at the center. The anamorph has been described by Rogers (1985), but we were unable to confirm the presence of conidial structures when we studied the strain more than 30 years later.

**Secondary metabolites.** Stromata contain BNT and cohaerin type azaphilones according to the MS/MS analysis.

**Notes.** We were not only able to confirm the morphometric results of Ju and Rogers (1996) but even established that this species is characterized by a rather specific metabolite profile. This species has to our knowledge still not been reported from outside America and seems to be most frequently encountered in the Eastern USA.

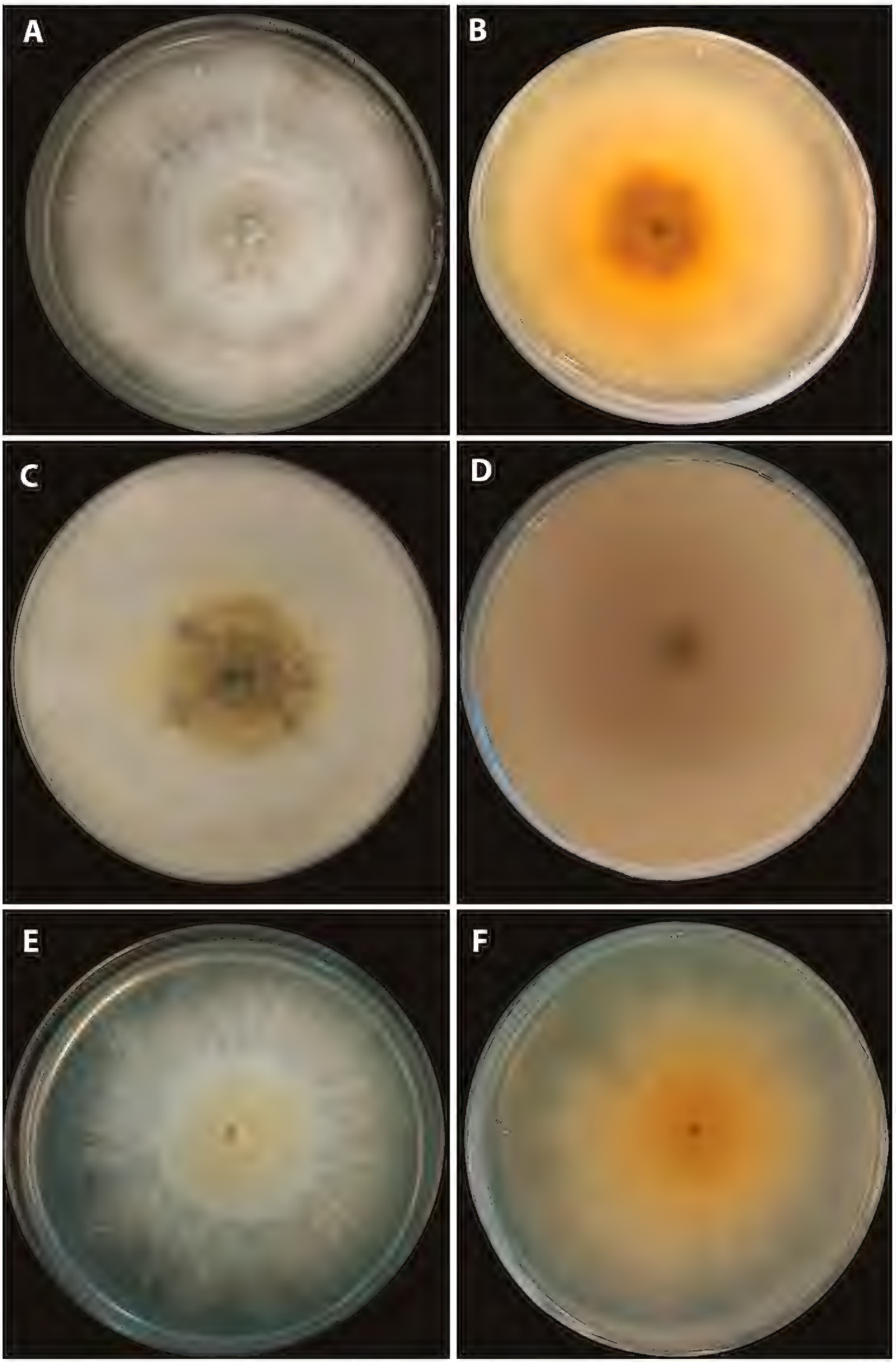


**Figure 4.** *Parahypoxylon papillatum* comb. nov. (ATCC 58729) Colonies after 2 weeks (**A, B**) on 2% MEA (**C, D**) on OA (**E, F**) on YM.

**Further specimens examined.** USA. Kansas, on decorticated wood, Feb 1884, F.W. Cragin 257 (NY00830462, syntype of *H. papillatum*); Pennsylvania, Allegheny Co., on dead wood, 14 Aug 1941, Henry, L.K. 4885 (BPI 591033); Pennsylvania, Meadville, old log, 17 Oct 1922, E.C. Smith 353 (BPI 591030); CANADA., on wood, J. Dearness (BPI 591035A, syntype of *H. papillatum*).

***Parahypoxylon ruwenzoriense*** **M. Cedeño-Sanchez, E. Charria-Girón & M. Stadler, sp. nov.**
MycoBank No: 845457
Figs 5–6

**Holotype.** Democratic Republic Of The Congo. North Kivu: Mt. Ruwenzori, about 00°33.961'N, 29°81.795'E, between 2,138 and 2,400 m alt., 3–5 Feb 2008, tropical mountain forest, C. Decock (MUCL 51392, ex-holotype culture MUCL 51392).

**Etymology.** Named after the Ruwenzori Mountains, where the species was collected.

**Teleomorph.** Stromata superficial, incomplete, effused-pulvinate, 60 mm long × 40 mm broad × 3–5 mm thick; surface Fawn (87), with inconspicuous perithecial mounds, with a black, shiny hard crust 100–150 µm thick above perithecia, without visible granules, with KOH-extractable pigments Hazel (88); the pruina hyphae turn violet in KOH; the tissue below the perithecia 2–4 mm thick, vertically fibrose, dark grey. Perithecia tubular, 0.90–1.50 mm high × 0.2–0.3 mm diam (n=18). Ostioles umbilicate, surrounded by a white substance. Asci cylindrical, 8-spored, the spore-bearing parts 82–105 µm long × 5.5–6.0 µm broad, the stipes 38–130 µm long, with amyloid, discoid apical ring 0.7–2.0 µm high × 2.5–3.5 µm (n=21) broad. Ascospores smooth, unicellular, brown to dark brown, narrowly ellipsoid, nearly equilateral with narrowly rounded ends, 10.5–13.8 × 4.0–5.6 µm (n=40), with a faint, straight germ slit; perispore indehiscent in 10% KOH.

**Cultures and anamorph.** Colonies on MEA, OA, and YM covering a 9 cm Petri plate in 2 weeks, with mycelium white at first, flat to raised in some zones, to becoming greenish in the center. Reverse at first yellowish, to become orange with a black spot at the center. Conidiophores not produced.

**Secondary metabolites.** Stromata contain BNT and cohaerin type azaphilones according to the MS/MS analysis.

**Notes.** *P. ruwenzoriense* is phylogenetically close to *P. papillatum* but differs by its KOH-extractable pigments Hazel (88) and by smaller ascospores.

## Metabolomic profiling of stromata

As explained in the Experimental section, stromata of five herbarium specimens assignable to *Parahypoxylon* were extracted and analysed by UHPLC-DAD-IM-MS/MS. The raw data sets were pre-processed and the obtained feature table dereplicated using high resolution *m/z*, MS/MS spectra, retention time, CCS value, and UV/Vis spectra and reference data obtained from our in-house library of common secondary metabolites of the Hypoxylaceae (data not shown).

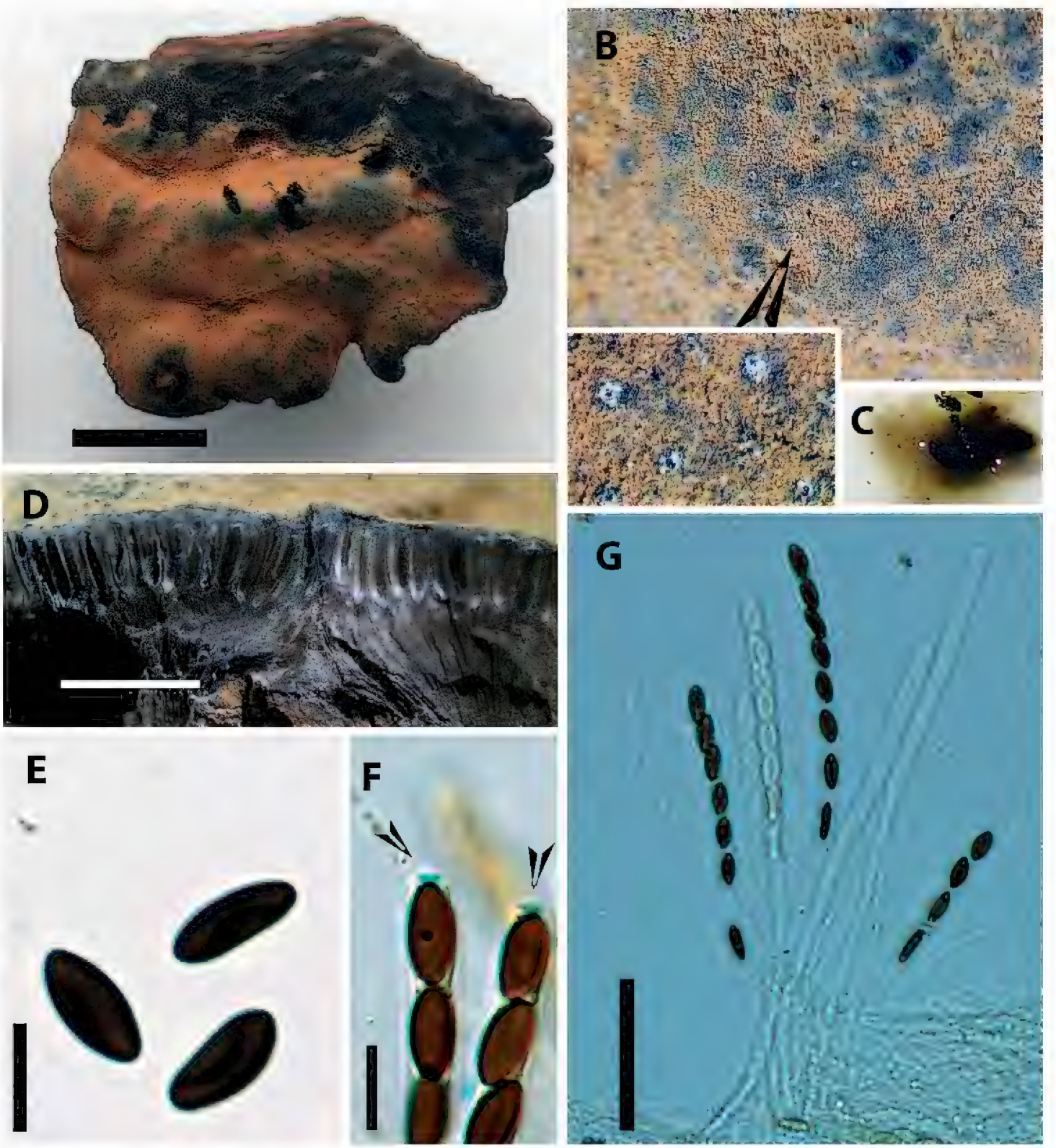


**Figure 5.** *Parahypoxylon ruwenzoriense* sp. nov. (MUCL 51392). **A** stroma **B** ostioles with white ring **C** KOH extractable stromatal pigments **D** perithecia (cross section) **E** ascospores **F** amyloid apical apparatus (blueing in Melzer's reagent) indicated by arrowheads **G** asci. Scale bars: 1 cm (**A**); 2 mm (**D**); 10 µm (**E, F**); 50 µm (**G**).

From the base peak chromatograms (BPC) of the stromatal extracts of the studied specimens, six major peaks could be distinguished (Fig. 7). An additional MS/MS similarity search without matching the precursor mass against our in-house library in MetaboScape yielded a MS/MS score > 700 for compounds **2** and **5** when compared with cohaerin E, cohaerin H, and minutellin A standards, which were not contained in the stromatal extracts (Suppl. material 1: fig. S2). This tentatively advocated

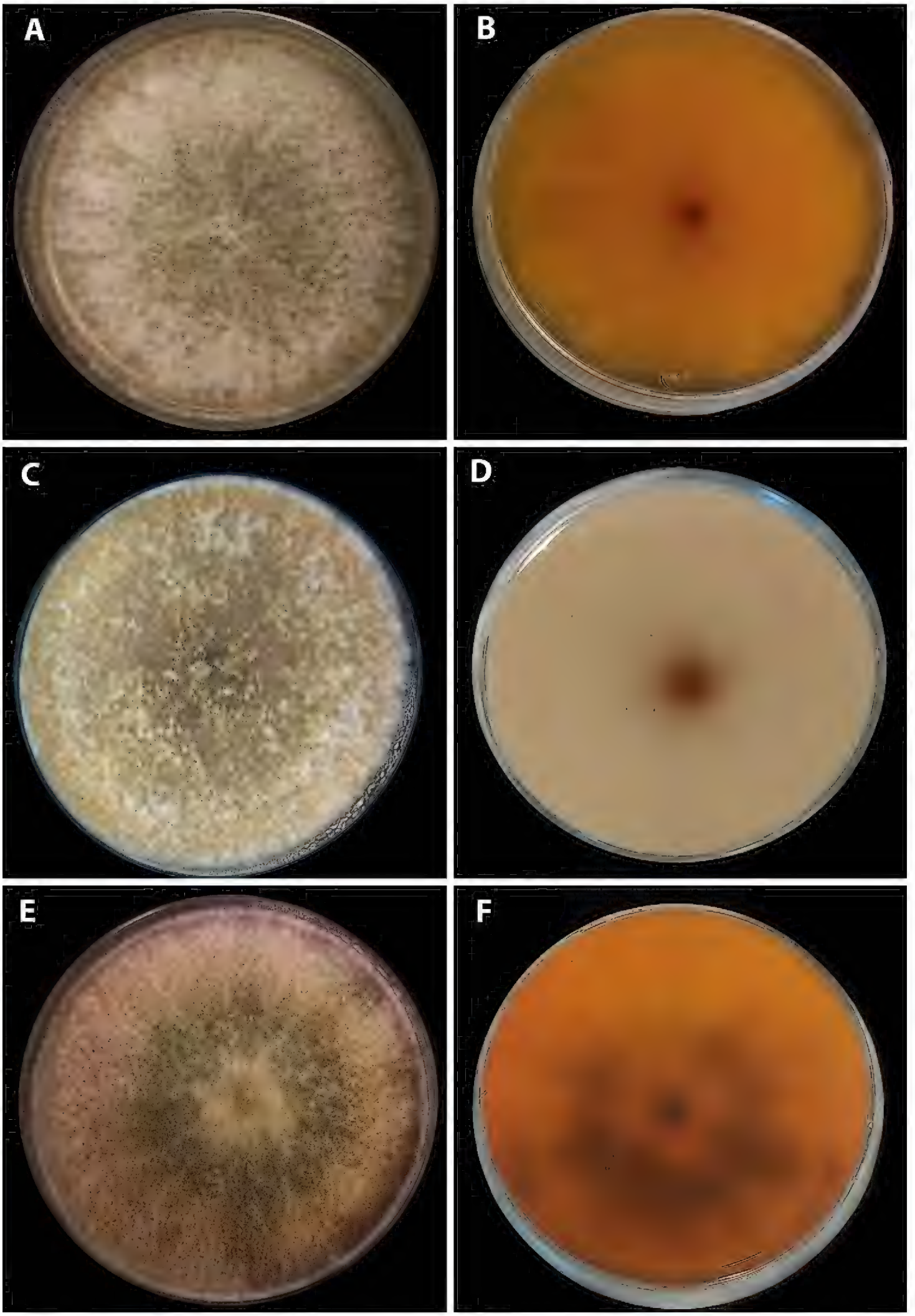


**Figure 6.** *Parahypoxylon ruwenzoriense* sp. nov. (MUCL 51392) Colonies after 2 weeks (**A, B**) on 2% MEA (**C, D**) on OA (**E, F**) on YM.

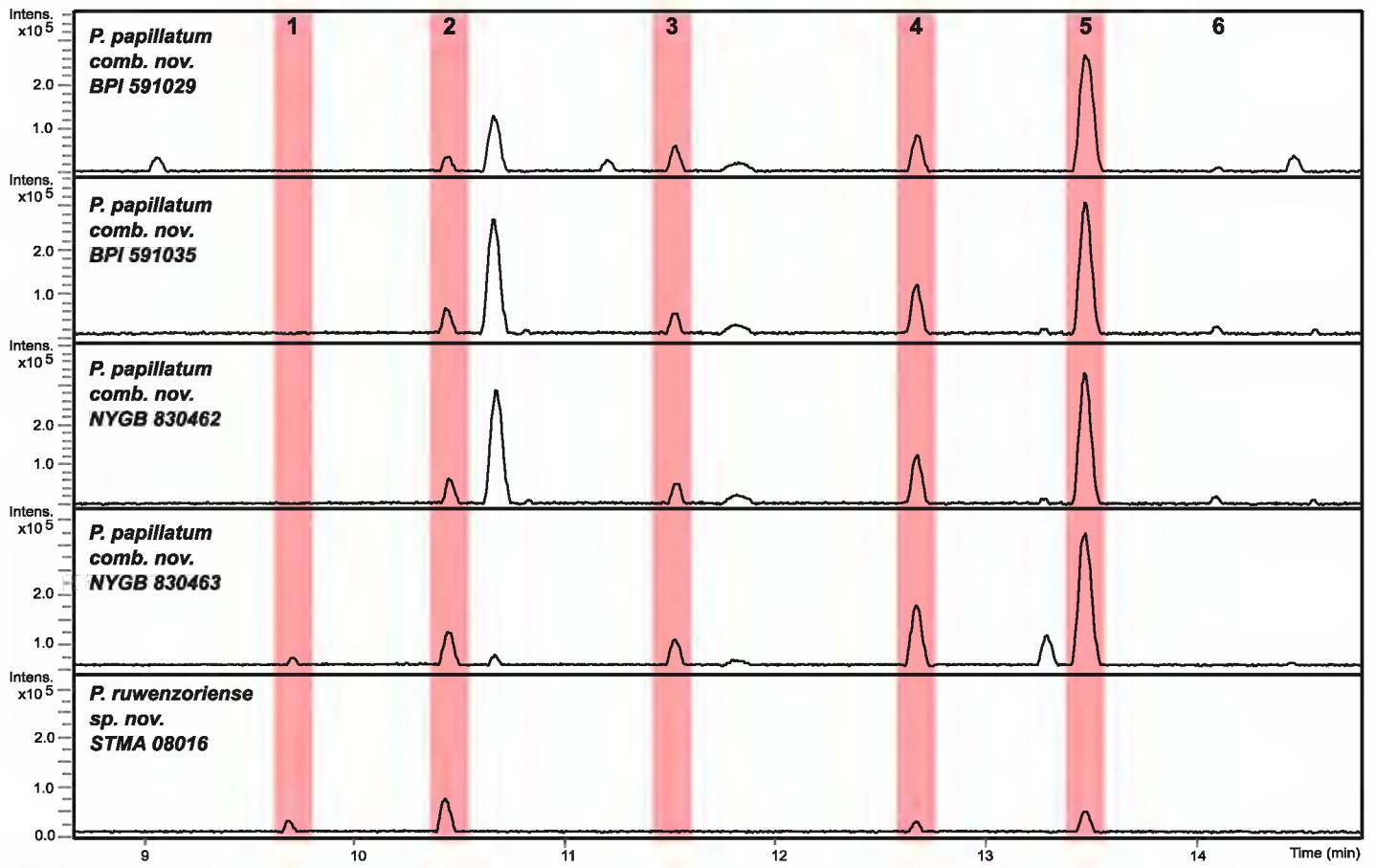


**Figure 7.** Base peak chromatograms (BPCs) from UHPLC-MS analysis of the stromatal extracts of *P. papillatum* (BPI 591029), *P. papillatum* (BPI 591035), *P. papillatum* (NYGB 830462), *P. papillatum* (NYGB 830463), and *Parahypoxylon ruwenzoriense* sp. nov. (STMA 08016). Compounds common between several species (numbered **1–6**) are highlighted in red.

a structural relation to the azaphilone family (Fig. 8a). Molecular formulae for compounds **1–6** were predicted as $C_{23}H_{24}O_7$, $C_{23}H_{22}O_7$, $C_{23}H_{20}O_8$, $C_{23}H_{22}O_6$, $C_{23}H_{20}O_6$, and $C_{23}H_{21}NO_5$ (Suppl. material 1: table S7), with a lower number of carbons than cohaerin E ($C_{28}H_{30}O_6$), cohaerin H ($C_{28}H_{32}O_6$), and minutellin A ($C_{28}H_{30}O_7$). To further validate the presence of cohaerin E-like azaphilones in the stromatal extracts of the *Parahypoxylon* spp. a molecular networking (MN) approach was pursued. The above mentioned tool can be employed to organize in an automatic basis MS/MS spectra into groups based on similarities in their fragmentation patterns and the hypothesis that structurally related molecules will yield similar MS/MS spectra (Duncan et al. 2015). For this analysis, we compared the MS/MS spectra of cohaerin E, cohaerin H, and minutellin A (Suppl. material 1: table S7, fig. S2) with all MS/MS spectra obtained from the *Parahypoxylon* gen. nov. stromatal extracts by means of the unsupervised machine learning approach Spec2Vec. As a result, the molecular cluster containing the cohaerin standards consisted of 29 consensus spectra (nodes), which included compounds **1–6** (Fig. 8b). In addition, cohaerin E and H have UV/Vis absorptions at $\lambda_{max}$ 226–223 and 344–380 nm, which are resembling UV/Vis absorptions from compounds **1**, **3**, **4**, and **6**. Minutellin A displayed UV/Vis absorptions at $\lambda_{max}$ 224, 271, and 343 nm, a pattern identified also for compounds **2** and **5** (Fig. 8c).

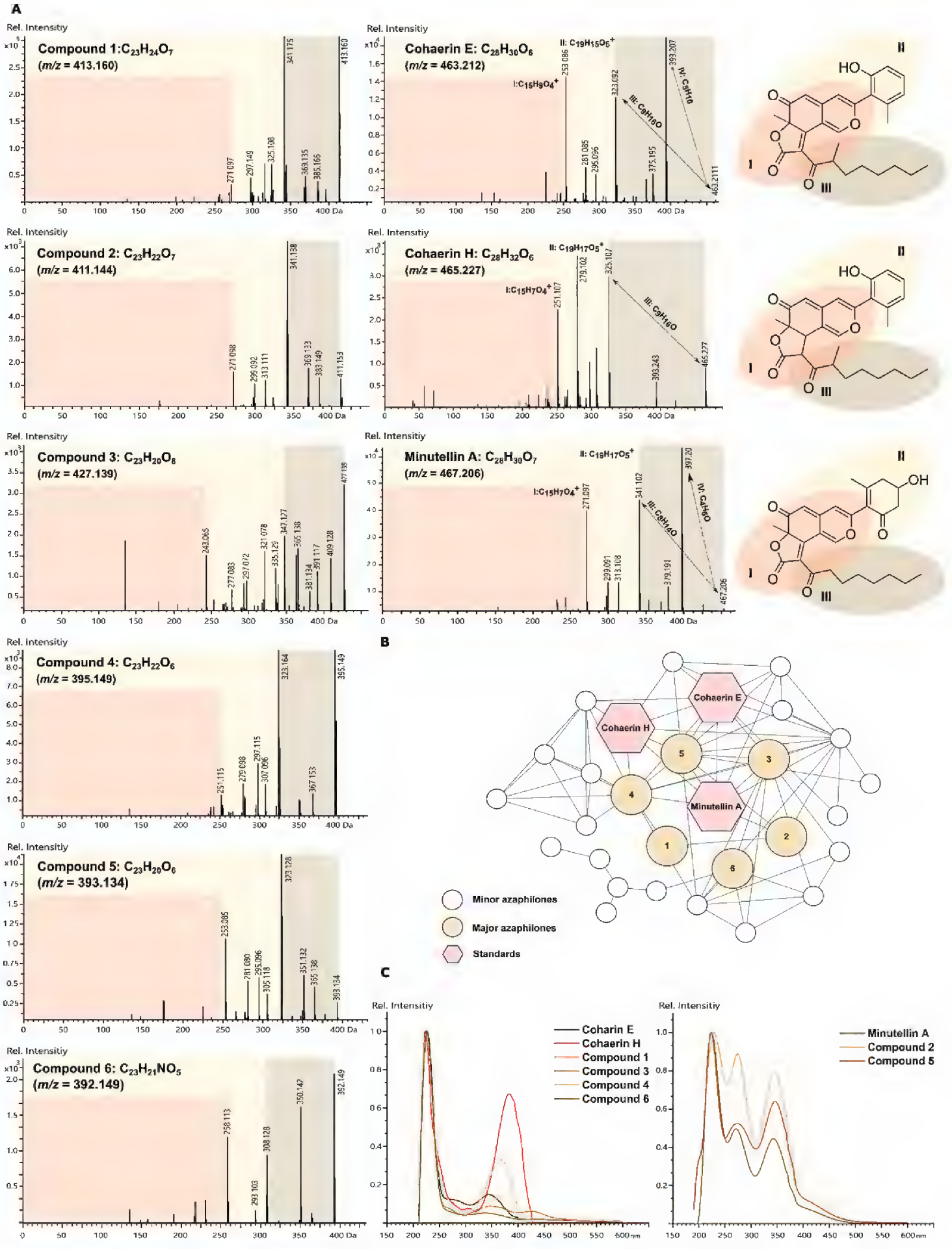


**Figure 8. A** Reference MS/MS spectra of cohaerin E, cohaerin H, and minutellin A standards, and the six major azaphilones identified in the UHPLC-MS chromatograms of stromatal extracts from the *Parahypoxylon* spp. **B** azaphilone cluster in a molecular network created from the *Parahypoxylon* spp. stromatal extracts and MS/MS spectra from selected standards **C** UV/Vis profile comparison from compound **1**–**6**, cohaerin E, cohaerin H, and minutellin A.

Cohaerin-type azaphilones present as well a distinct MS fragmentation pattern. In MS/MS experiments, cohaerin E generated fragment ions at 393.207 Da, 323.092 Da, 281.085 Da, and 253.086 Da, while minutellin A generated fragment ions at 397.201 Da, 341.102 Da, 299.091 Da, and 271.097 Da. The most abundant fragments were annotated using the CFM-ID 4.0 peak assignment module. In both cases, the most abundant fragments were traced down to the azaphilone backbone (Fig. 9). For instance, the mass difference of 18 Da between 323.092 Da and 341.102 Da could be interpreted as $H_2O$, reflecting the different substitution of the 3-methylphenol moiety. Fragment ions at 281.085 Da and 253.086 Da for cohaerin E represent the tricyclic portion of the molecule, while fragment ions at 299.091 Da and 271.097 Da represent the same part of the molecule in minutellin A. Analogously, MS fragmentation patterns for cohaerin H (Fig. 8) resembles the generated fragments for cohaerin E. As some typical cohaerin-type azaphilones fragmentation patterns were conserved, we assume that the changes found for the stromatal metabolites of **1–6** occur in the side chain of the molecules. In summary, the UHPLC-DAD-IM-MS/MS and UV/Vis data, combined with a comparison of molecular networking analyses, indicated the presence of novel azaphilones related to the cohaerin family in the stromatal extracts from the *Parahypoxylon* spp., in contrast to the absence of other common secondary metabolites of the Hypoxylaceae.

## Discussion

The genus *Hypoxylon* in the current taxonomic concept has frequently been shown to be paraphyletic (Wendt et al. 2018; Lambert et al. 2019), which has once more been confirmed in this study, foreshadowing again future rearrangements for a thorough revision of its systematics. This is especially apparent because the type species *H. fragiforme* forms a relatively small clade clustering with a small subset of closely related taxa. Therefore, further segregation will eventually be unavoidable once more data to safely delineate the different lineages becomes available. Here, we gathered chemotaxonomic, morphological and sequence data to enable a polyphasic characterization of a basal clade formerly phylogenetically resolved inside *Hypoxylon*, containing specimen closely related to *H. papillatum*, for which we propose the erection of the new genus *Parahypoxylon*, sharing many salient features with *Hypoxylon* in the "traditional" definition.

The investigation of the stromatal metabolite extracts by HPLC has proven to be a valuable resource to achieve a more natural classification of hypoxylaceous taxa (Kuhnert et al. 2015; Wendt et al. 2018; Lambert et al. 2019). Recent advances in the analytics for in-depth characterization of natural products, mainly driven by metabolomics-based strategies, have enabled a better understanding of complex natural systems (Van der Hooft et al. 2020). The current MS-based techniques can help as a predictor for the discovery of new carbon skeletons to help and prioritize their isolation

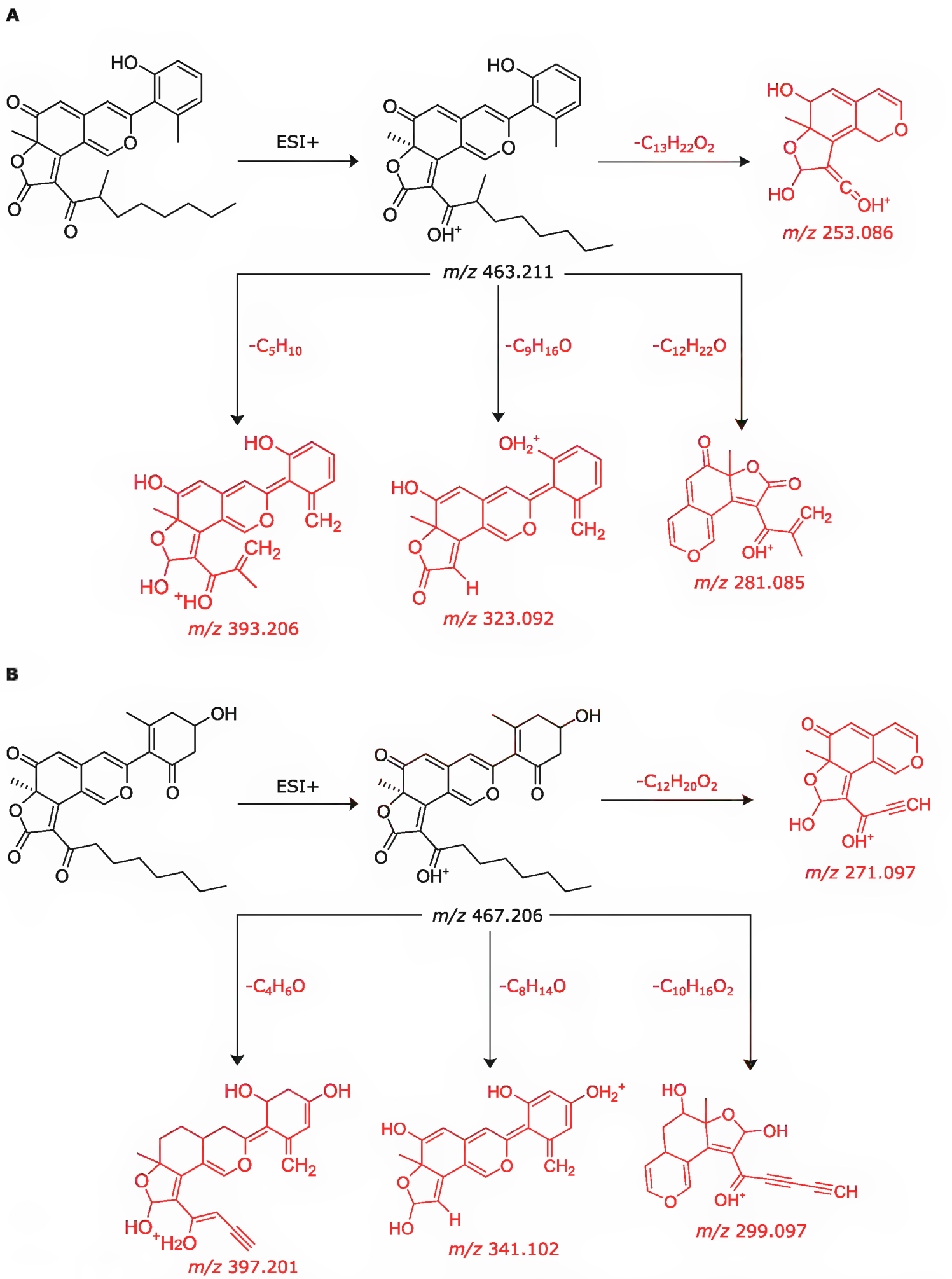


**Figure 9. A** most abundant fragment ions observed in MS/MS spectra for cohaerin E and associated structures as predicted by CFM-ID 4.0 **B** most abundant fragment ions observed in MS/MS spectrum for minutellin A and associated structures as predicted by CFM-ID 4.0.

and description instead of the isolation of new derivatives of already known metabolite scaffolds. Nevertheless, relying mainly on MS/MS fragmentation spectra could lead to an underestimation of chemical diversity. The complex chemical space produced by a single BGC may result in completely different fragmentation patterns only by the addition of small structural changes (McCaughey et al. 2022). Still, a general methodology for characterizing and classifying structural analogs with a common biosynthetic origin is absent particularly in the field of fungal natural products (Almeida et al. 2020).

However, in many occasions and applications, the isolation and structure elucidation of yet unidentified compounds is not possible, such as in the example of isolating pigments from natural sources, as is the case in the genus *Hypoxylon*. Even very old specimens have been reported to harbor intact secondary metabolites, as has been described for fossilized stromata assigned to *Hypoxylon fragiforme* in a study of archeological samples by Surup et al. (2018). Here, fortunately the original species could be recollected in German woods, but for rarer specimens, or specimens only producing scarce amounts of stromata, this is not a practicable option. Instability of the contained metabolites during e.g. purification further complicates the issue (Stadler et al. 2008; Kuhnert et al. 2014b; Sir et al. 2019). In this study, we demonstrated the value of integrating metabolomics-based tools to characterize the secondary metabolite profile of the type and authentic specimens of *P. papillatum* and the new species from the D.R. Congo.

An MS/MS analysis of the major metabolites suggested the presence of six unknown compounds assignable to the azaphilones related to the cohaerin family, which have been predicted to harbor a smaller carbon skeleton than the known cohaerins, and which still conserve some of the distinctive fragmentation patterns of these secondary metabolites (Suppl. material 1: fig. S3). This phenomenon has been exemplified within the Hypoxylaceae, which present a highly diverse group of PKS-derived pigments, among which the different subfamilies present different attached side chains at the C-8 oxygen (Kuhnert et al. 2021). The above findings suggest that the type of azaphilone produced by the studied species belong to a different type of azaphilones with a shorter side chain, but with a shared backbone in comparison to the cohaerins and minutellins. Additionally, the number of nodes found in the MN analysis suggests that the chemical diversity of the azaphilones produced by the strains belonging to *Parahypoxylon* gen. nov. is much higher than thought. In general, following a similar approach, the MolNetEnhancer workflow allowed the characterization of triterpenoid metabolites with several distinct phenolic acid modifications (e.g., vanillate, protocatechuate) in a different taxonomic background in the plant family Rhamnaceae (Ernst et al. 2019). The same methodology enabled the annotation of molecular families with known chemical motifs previously unreported for *Salinispora*, *Streptomyces*, and *Xenorhabdus* bacterial extracts (Ernst et al. 2019). Even though the ideal scenario would remain to isolate and elucidate the structures of the secondary metabolites, these tools are a powerful resource to classify chemical structural annotation and enhance our understanding of chemodiversity by adding biological and chemical insights of complex metabolic mixtures. It is worth noting that the stromatal material could eventually become available in the future from forthcoming collection campaigns, and

therefore the aforementioned hypothesis might be confirmed through isolation and chemical characterization of the major metabolites.

In this context, the stromatal metabolite profile of the specimens of *P. papillatum* and the new species *P. ruwenzoriense* are rather unique, even though it exhibits related chemotaxonomic features more likely to be found in the Hypoxylaceae. The cohaerin type azaphilones (which include also the multiformins and minutellins) have first been reported by Quang et al. (2005a, b, 2006), Surup et al. (2013) and Kuhnert et al. (2017b) and were recently found to possess interesting antiviral effects (Jansen-Olliges et al. 2023). Their producers are now all classified in *Jackrogersella* (Wendt et al. 2018) and were formerly placed in *Hypoxylon* sect. *Annulata* or (Ju and Rogers 1996) *Annulohypoxylon* (Hsieh et al. 2005), respectively. Kuhnert et al. (2017a) already reported that the species of *Annulohypoxylon* are divided into two chemotypes, one of which is characterized by stromata with papillate ostioles and cohaerin type azaphilones. The other chemotype is devoid of these compounds and produces binaphthalenes as prevailing stromatal metabolites. It includes *A. truncatum*, the type species of *Annulohypoxylon*, and many other species that feature ostiolar discs. Since this coincided with the molecular phylogeny by Wendt et al. (2018), the new genus *Jackrogersella* was erected for the cohaerin-containing species with papillate, diskless ostioles. There is only one species in *Annulohypoxylon* (i.e., *A. michelianum*) that has such ostiolar rings and also produces cohaerins. It was left at interim in *Annulohypoxylon*, even though its DNA sequence occupied a separate clade in the phylogeny by Wendt et al. (2018). The reason is that the strain studied did not constitute type material, and we felt that the erection of a separate genus should only be carried out by including fresh material from the geographic area and host (*Laurus* in South Europe) from which the holotype specimen was reported. Aside from the above-mentioned fungi, metabolites with cohaerin-like characteristics (i.e. characteristic mass and diode array spectra) have even been detected in species of *Hypoxylon*, such as *H. pulicicidum* (Bills et al. 2012). A recent study based on the analysis of full genomes based on 3$^{rd}$ generation sequencing techniques, such as PacBio and Oxford nanopore (Wibberg et al. 2021), has even revealed the corresponding biosynthetic gene clusters encoding for these azaphilone pigments to be present in the studied *Jackrogersella* species and *H. pulicicidum* (Kuhnert et al. 2021). For instance, the identified BGC in *H. pulicicidum* carries the core set of conserved genes for this family of azaphilones, but the additional presence of additional tailoring enzymes indicates that the produced metabolites might have different structural features compared to the known cohaerins (Kuhnert et al. 2021).

In the future, it will become easier to tell if the genetic information for the successful biosynthesis of such secondary metabolites is present in the genomes of the respective organisms even if the products cannot be detected. Chemotaxonomic evidence can also be used to segregate the new genus from the species that are located in neighboring basal clades in the current phylogeny (i.e., *Hypoxylon aeruginosum* and *Durotheca* spp.). Interestingly, these species neither contain azaphilones nor binaphthalenes, with *H. aeruginosum* and the related genus *Chlorostroma* reported to have lepraric acid derivatives as major stromatal metabolites (Læssøe et al. 2010), which are

otherwise unique and only occur in some lichenized ascomycetes. *Durotheca*, on the other hand, appears to be poor in stromatal metabolites, and Læssøe et al. (2013) only found traces of lepraric acids in one of the species they studied. The current study has further confirmed the results by de Long et al. (2019), who found that *Durotheca* is a hypoxylaceous genus, even though its species have a distinctive ascospore morphology and other secondary metabolites.

The integration of state-of-the-art metabolomic-based tools in chemotaxonomic surveys will further accelerate and assist the systematic study of paraphyletic taxa within the concept of polyphasic taxonomy as herein demonstrated for the introduction of *Parahypoxylon*.

## Acknowledgements

This work was funded by the DFG (Deutsche Forschungsgemeinschaft) priority program "Taxon-Omics: New Approaches for Discovering and Naming Biodiversity" (SPP 1991). It also benefited from the European Union's H2020 Research and Innovation Staff Exchange program (RISE) [Grant No. 101008129: MYCOBIOMICS], granted to J.J. Luangsa-ard and M. Stadler. MCS gratefully acknowledges a PhD stipend from The National Secretariat of Science, Technology and Innovation of the Republic of Panama (SENACYT) and the Institute for the Development of Human Resources (IFARHU). E. Charria-Girón was funded by the HZI POF IV Cooperativity and Creativity Project Call. Additionally, we gratefully acknowledge support from the curators of the international herbaria, above all Lisa A Castlebury (BPI), Laura Briscoe (NY) and Monique Slipher (WSP), who provided important specimens for this study. Additionally, we are grateful for the expert and technical advice from Ulrike Beutling and Frank Surup.

## References

Almeida H, Palys S, Tsang A, Diallo AB (2020) TOUCAN: A framework for fungal biosynthetic gene cluster discovery. NAR Genomics and Bioinformatics 2(4): 1–11. https://doi.org/10.1093/nargab/lqaa098

Anisimova M, Gil M, Dufayard JF, Dessimoz C, Gascuel O (2011) Survey of branch support methods demonstrates accuracy, power, and robustness of fast likelihood-based approximation schemes. Systematic Biology 60(5): 685–699. https://doi.org/10.1093/sysbio/syr041

Becker K, Stadler M (2021) Recent progress in biodiversity research on the Xylariales and their secondary metabolism. The Journal of Antibiotics 74(1): 1–23. https://doi.org/10.1038/s41429-020-00376-0

Becker K, Lambert C, Wieschhaus J, Stadler M (2020) Phylogenetic assignment of the fungicolous *Hypoxylon invadens* (Ascomycota, Xylariales) and investigation of its secondary metabolites. Microorganisms 8(9): 1397. https://doi.org/10.3390/microorganisms8091397

Bills GF, González-Menéndez V, Martín J, Platas G, Fournier J, Peršoh D, Stadler M (2012) *Hypoxylon pulicicidum* sp. nov. (Ascomycota, Xylariales), a pantropical insecticide-producing endophyte. PLoS ONE 7(10): e46687. https://doi.org/10.1371/journal.pone.0046687

Bitzer J, Læssøe T, Fournier J, Kummer V, Decock C, Tichy H-V, Piepenbring M, Peršoh D, Stadler M (2008) Affinities of *Phylacia* and the daldinoid Xylariaceae, inferred from chemotypes of cultures and ribosomal DNA sequences. Mycological Research 112(2): 251–270. https://doi.org/10.1016/j.mycres.2007.07.004

Cedeño-Sanchez M, Wendt L, Stadler M, Mejía LC (2020) Three new species of *Hypoxylon* and new records of Xylariales from Panama. Mycosphere 11(1): 1457–1476. https://doi.org/10.5943/mycosphere/11/1/9

Chernomor O, Von Haeseler A, Minh BQ (2016) Terrace aware data structure for phylogenomic inference from supermatrices. Systematic Biology 65(6): 997–1008. https://doi.org/10.1093/sysbio/syw037

Daranagama DA, Camporesi E, Tian Q, Liu X, Chamyuang S, Stadler M, Hyde KD (2015) *Anthostomella* is polyphyletic comprising several genera in Xylariaceae. Fungal Diversity 73(1): 203–238. https://doi.org/10.1007/s13225-015-0329-6

Daranagama DA, Hyde KD, Sir EB, Thambugala KM, Tian Q, Samarakoon MC, McKenzie EHC, Jayasiri SC, Tibpromma S, Bhat JD, Liu X, Stadler M (2018) Towards a natural classification and backbone tree for Graphostromataceae, Hypoxylaceae, Lopadostomataceae and Xylariaceae. Fungal Diversity 88(1): 1–165. https://doi.org/10.1007/s13225-017-0388-y

de Long Q, Liu LL, Zhang X, Wen TC, Kang JC, Hyde KD, Shen XC, Li QR (2019) Contributions to species of Xylariales in China-1. *Durotheca* species. Mycological Progress 18(3): 495–510. https://doi.org/10.1007/s11557-018-1458-6

Duncan KR, Crüsemann M, Lechner A, Sarkar A, Li J, Ziemert N, Wang M, Bandeira N, Moore BS, Dorrestein PC, Jensen PR (2015) Molecular networking and pattern-based genome mining improves discovery of biosynthetic gene clusters and their products from *Salinispora* species. Chemistry & Biology 22(4): 460–471. https://doi.org/10.1016/j.chembiol.2015.03.010

Ernst M, Kang K, Caraballo-Rodríguez AM, Nothias L-F, Wandy J, Chen C, Wang M, Rogers S, Medema MH, Dorrestein PC, van der Hooft JJJ (2019) Molnetenhancer: Enhanced molecular networks by integrating metabolome mining and annotation tools. Metabolites 9(7): 144. https://doi.org/10.3390/metabo9070144

Felsenstein J (1985) Confidence limits on phylogenies: An approach using the bootstrap. Evolution 39(4): 783–791. https://doi.org/10.2307/2408678

Fournier J, Köpcke B, Stadler M (2010a) New species of *Hypoxylon* from western Europe and Ethiopia. Mycotaxon 113(1): 209–235. https://doi.org/10.5248/113.209

Fournier J, Stadler M, Hyde KD, Duong LM (2010b) The new genus *Rostrohypoxylon* and two new *Annulohypoxylon* species from Northern Thailand. Fungal Diversity 40(1): 23–36. https://doi.org/10.1007/s13225-010-0026-4

Fournier J, Flessa F, Peršoh D, Stadler M (2011) Three new *Xylaria* species from Southwestern Europe. Mycological Progress 10(1): 33–52. https://doi.org/10.1007/s11557-010-0671-8

Friebes G, Wendelin I (2016) Studies on *Hypoxylon ferrugineum* (Xylariaceae), a rarely reported species collected in the urban area of Graz (Austria). Ascomycete.org 8: 83–90.

Helaly SE, Thongbai B, Stadler M (2018) Diversity of biologically active secondary metabolites from endophytic and saprotrophic fungi of the ascomycete order Xylariales. Natural Product Reports 35(9): 992–1014. https://doi.org/10.1039/C8NP00010G

Heredia G, Li DW, Wendt L, Réblová M, Arias RM, Gamboa-Angulo M, Štěpánek V, Stadler M, Castañeda-Ruíz RF (2020) *Natonodosa speciosa* gen. et sp. nov. and rediscovery of *Poroisariopsis inornata*: Neotropical anamorphic fungi in Xylariales. Mycological Progress 19(1): 15–30. https://doi.org/10.1007/s11557-019-01537-8

Hsieh H-M, Ju Y-M, Rogers JD (2005) Molecular phylogeny of *Hypoxylon* and closely related genera. Mycologia 97(4): 844–865. https://doi.org/10.1080/15572536.2006.11832776

Hsieh H-M, Lin C-R, Fang M-J, Rogers JD, Fournier J, Lechat C, Ju Y-M (2010) Phylogenetic status of *Xylaria* subgenus *Pseudoxylaria* among taxa of the subfamily Xylarioideae (Xylariaceae) and phylogeny of the taxa involved in the subfamily. Molecular Phylogenetics and Evolution 54(3): 957–969. https://doi.org/10.1016/j.ympev.2009.12.015

Huber F, Ridder L, Verhoeven S, Spaaks JH, Diblen F, Rogers S, Van Der Hooft JJJ (2021) Spec2Vec: Improved mass spectral similarity scoring through learning of structural relationships. PLoS Computational Biology 17(2): e1008724. https://doi.org/10.1371/journal.pcbi.1008724

Hyde K, Norphanphoun C, Maharachchikumbura SSN, Bhat DJ, Jones EBG, Bundhun D, Chen YJ, Bao DF, Boonmee S, Calabon MS, Chaiwan N, Chethana KWT, Dai DQ, Dayarathne MC, Devadatha B, Dissanayake AJ, Dissanayake LS, Doilom M, Dong W, Fan XL30 , Goonasekara ID, Hongsanan S, Huang SK, Jayawardena RS, Jeewon R, Karunarathna A, Konta S, Kumar V, Lin CG, Liu JK, Liu NG, Luangsa-ard J, Lumyong S, Luo ZL, Marasinghe DS, McKenzie EHC, Niego AGT, Niranjan M, Perera RH, Phukhamsakda C, Rathnayaka AR, Samarakoon MC, Samarakoon SMBC, Sarma VV, Senanayake IC, Shang QJ, Stadler M, Tibpromma S, Wanasinghe DN, Wei DP, Wijayawardene NN, Xiao YP, Yang J, Zeng XY, Zhang SN, Xiang MM (2020) Refined families of Sordariomycetes. Mycosphere 11(1): 305–1059. https://doi.org/10.5943/mycosphere/11/1/7

Jansen-Olliges L, Chatterjee S, Jia L, Stahl F, Bär C, Stadler M, Surup F, Zeilinger C (2022) Cohaerin-type azaphilones prevent SARS-CoV-2 binding to ACE2 receptor. Cells 12(1): 83. https://doi.org/10.3390/cells12010083

Ju Y, Rogers JD (1996) A revision of the genus *Hypoxylon*. Mycologia Memoir No. 20. American Phytopathological Society, APS Press.

Ju Y-M, Rogers JD, Hsieh H-M (2003) The genus *Theissenia*: *T. pyrenocrata*, *T. cinerea* sp. nov., and *T. eurima* sp. nov. Mycologia 95(1): 109–116. https://doi.org/10.1080/15572536.2004.11833138

Ju Y-M, Hsieh H-M, Ho M-C, Szu D-H, Fang M-J (2007) *Theissenia rogersii* sp. nov. and phylogenetic position of *Theissenia*. Mycologia 99(4): 612–621. https://doi.org/10.1080/15572536.2007.11832555

Kalyaanamoorthy S, Minh BQ, Wong TKF, von Haeseler A, Jermiin LS (2017) ModelFinder: Fast model selection for accurate phylogenetic estimates. Nature Methods 14(6): 587–589. https://doi.org/10.1038/nmeth.4285

Katoh K, Rozewicki J, Yamada KD (2019) MAFFT online service: Multiple sequence alignment, interactive sequence choice and visualization. Briefings in Bioinformatics 20(4): 1160–1166. https://doi.org/10.1093/bib/bbx108

Kearse M, Moir R, Wilson A, Stones-Havas S, Cheung M, Sturrock S, Buxton S, Cooper A, Markowitz S, Duran C, Thierer T, Ashton B, Meintjes P, Drummond A (2012) Geneious Basic: An integrated and extendable desktop software platform for the organization and analysis of sequence data. Bioinformatics 28(12): 1647–1649. https://doi.org/10.1093/bioinformatics/bts199

Koukol O, Kelnarová I, Černý K (2015) Recent observations of sooty bark disease of sycamore maple in Prague (Czech Republic) and the phylogenetic placement of *Cryptostroma corticale*. Forest Pathology 45(1): 21–27. https://doi.org/10.1111/efp.12129

Kuhnert E, Heitkämper S, Fournier J, Surup F, Stadler M (2014a) Hypoxyvermelhotins A–C, new pigments from *Hypoxylon lechatii* sp. nov. Fungal Biology 118(2): 242–252. https://doi.org/10.1016/j.funbio.2013.12.003

Kuhnert E, Fournier J, Peršoh D, Luangsa-ard JJD, Stadler M (2014b) New *Hypoxylon* species from Martinique and new evidence on the molecular phylogeny of *Hypoxylon* based on ITS rDNA and β-tubulin data. Fungal Diversity 64(1): 181–203. https://doi.org/10.1007/s13225-013-0264-3

Kuhnert E, Surup F, Sir EB, Lambert C, Hyde KD, Hladki AI, Romero AI, Stadler M (2015) Lenormandins A—G, new azaphilones from *Hypoxylon lenormandii* and *Hypoxylon jaklitschii* sp. nov., recognised by chemotaxonomic data. Fungal Diversity 71(1): 165–184. https://doi.org/10.1007/s13225-014-0318-1

Kuhnert E, Sir EB, Lambert C, Hyde KD, Hladki AI, Romero AI, Rohde M, Stadler M (2017a) Phylogenetic and chemotaxonomic resolution of the genus *Annulohypoxylon* (Xylariaceae) including four new species. Fungal Diversity 85(1): 1–43. https://doi.org/10.1007/s13225-016-0377-6

Kuhnert E, Surup F, Halecker S, Stadler M (2017b) Minutellins A – D, azaphilones from the stromata of *Annulohypoxylon minutellum* (Xylariaceae). Phytochemistry 137: 67–71. https://doi.org/10.1016/j.phytochem.2017.02.014

Kuhnert E, Navarro-Muñoz JC, Becker K, Stadler M, Collemare J, Cox RJ (2021) Secondary metabolite biosynthetic diversity in the fungal family Hypoxylaceae and *Xylaria hypoxylon*. Studies in Mycology 99(1): 100118. https://doi.org/10.1016/j.simyco.2021.100118

Læssøe T, Srikitikulchai P, Fournier J, Köpcke B, Stadler M (2010) Lepraric acid derivatives as chemotaxonomic markers in *Hypoxylon aeruginosum*, *Chlorostroma subcubisporum* and *C. cyaninum*, sp. nov. Fungal Biology 114(5–6): 481–489. https://doi.org/10.1016/j.funbio.2010.03.010

Læssøe T, Srikitikulchai P, Luangsa-ard JJD, Stadler M (2013) *Theissenia* reconsidered, including molecular phylogeny of the type species *T. pyrenocrata* and a new genus *Durotheca* (Xylariaceae, Ascomycota). IMA Fungus 4(1): 57–69. https://doi.org/10.5598/imafungus.2013.04.01.07

Lambert C, Wendt L, Hladki AI, Stadler M, Sir EB (2019) *Hypomontagnella* (Hypoxylaceae): A new genus segregated from *Hypoxylon* by a polyphasic taxonomic approach. Mycological Progress 18(1–2): 187–201. https://doi.org/10.1007/s11557-018-1452-z

Lambert C, Pourmoghaddam MJ, Cedeño-Sanchez M, Surup F, Khodaparast SA, Krisai-Greilhuber I, Voglmayr H, Stradal TEB, Stadler M (2021) Resolution of the *Hypoxylon fuscum* complex (Hypoxylaceae, Xylariales) and discovery and biological characterization of two of its prominent secondary metabolites. Journal of Fungi 7(2): 131. https://doi.org/10.3390/jof7020131

Lanfear R, Frandsen PB, Wright AM, Senfeld T, Calcott B (2016) PartitionFinder 2: New methods for selecting partitioned models of evolution for molecular and morphological phylogenetic analyses. Molecular Biology and Evolution 34: 772–773. https://doi.org/10.1093/molbev/msw260

Liu YJ, Whelen S, Hall BD (1999) Phylogenetic relationships among ascomycetes: Evidence from an RNA polymerase II subunit. Molecular Biology and Evolution 16(12): 1799–1808. https://doi.org/10.1093/oxfordjournals.molbev.a026092

Ma H, Song Z, Pan X, Li Y, Yang Z, Qu Z (2022) Multi-gene phylogeny and taxonomy of *Hypoxylon* (Hypoxylaceae, Ascomycota) from China. Diversity (Basel) 14(1): 37. https://doi.org/10.3390/d14010037

Matio Kemkuignou B, Schweizer L, Lambert C, Anoumedem EGM, Kouam SF, Stadler M, Marin-Felix Y (2022) New polyketides from the liquid culture of *Diaporthe breyniae* sp. nov. (Diaporthales, Diaporthaceae). MycoKeys 90: 85–118. https://doi.org/10.3897/mycokeys.90.82871

McCaughey CS, van Santen JA, van der Hooft JJJ, Medema MH, Linington RG (2022) An isotopic labeling approach linking natural products with biosynthetic gene clusters. Nature Chemical Biology 18(3): 295–304. https://doi.org/10.1038/s41589-021-00949-6

Miller JH (1961) A monograph of the world species of *Hypoxylon*. Univ. Georgia Press, Athens, 158 pp.

Minh BQ, Schmidt HA, Chernomor O, Schrempf D, Woodhams MD, von Haeseler A, Lanfear R (2020) IQ-TREE 2: New models and efficient methods for phylogenetic inference in the genomic era. Molecular Biology and Evolution 37(5): 1530–1534. https://doi.org/10.1093/molbev/msaa015

Nothias LF, Petras D, Schmid R, Dührkop K, Rainer J, Sarvepalli A, Protsyuk I, Ernst M, Tsugawa H, Fleischauer M, Aicheler F, Aksenov AA, Alka O, Allard PM, Barsch A, Cachet X, Caraballo-Rodriguez AM, Da Silva RR, Dang T, Garg N, Gauglitz JM, Gurevich A, Isaac G, Jarmusch AK, Kameník Z, Kang K, Kessler N, Koester I, Korf A, Le Gouellec A, Ludwig M, Martin H C, McCall L-I, McSayles J, Meyer SW, Mohimani H, Morsy M, Moyne O, Neumann S, Neuweger H, Nguyen NH, Nothias-Esposito M, Paolini J, Phelan VV, Pluskal T, Quinn RA, Rogers S, Shrestha B, Tripathi A, van der Hooft JJJ, Vargas F, Weldon KC, Witting M, Yang H, Zhang Z, Zubeil F, Kohlbacher O, Böcker S, Alexandrov T, Bandeira N, Wang M, Dorrestein PC (2020) Feature-based molecular networking in the GNPS analysis environment. Nature Methods 17(9): 905–908. https://doi.org/10.1038/s41592-020-0933-6

O'Donnell K, Cigelnik E (1997) Two divergent intragenomic rDNA ITS2 types within a monophyletic lineage of the fungus *Fusarium* are nonorthologous. Molecular Phylogenetics and Evolution 7(1): 103–116. https://doi.org/10.1006/mpev.1996.0376

Pourmoghaddam MJ, Lambert C, Surup F, Khodaparast SA, Krisai-Greilhuber I, Voglmayr H, Stadler M (2020) Discovery of a new species of the *Hypoxylon rubiginosum* complex from Iran and antagonistic activities of *Hypoxylon* spp. against the Ash Dieback pathogen, *Hymenoscyphus fraxineus*, in dual culture. MycoKeys 66: 105–133. https://doi.org/10.3897/mycokeys.66.50946

Quang DN, Hashimoto T, Nomura Y, Wollweber H, Hellwig V, Fournier J, Stadler M, Asakawa Y (2005a) Cohaerins A and B, azaphilones from the fungus *Hypoxylon cohaerens*,

and comparison of HPLC-based imetabolite profiles in *Hypoxylon* sect. *Annulata*. Phytochemistry 66: 797–809. 1 https://doi.org/10.1016/j.phytochem.2005.02.006

Quang DN, Hashimoto T, Stadler M, Radulović N, Asakawa Y (2005b) Antimicrobial azaphilones from the fungus *Hypoxylon multiforme*. Planta Medica 71(11): 1058–1062. https://doi.org/10.1055/s-2005-873129

Quang DN, Stadler M, Fournier J, Tomita A, Hashimoto T (2006) Cohaerins C–F, four azaphilones from the xylariaceous fungus *Annulohypoxylon cohaerens*. Tetrahedron 62(26): 6349–6354. https://doi.org/10.1016/j.tet.2006.04.040

Rayner RW (1970) A Mycological Colour Chart. Commonwealth Mycological Institute, Kew and British Mycological Society.

Rogers J (1985) *Hypoxylon duranii* sp. nov. and the anamorphs of *H. caries*, *H. papillatum*, and *Rosellinia subiculata*. Mycotaxon 23: 429–437.

Ronquist F, Teslenko M, van der Mark P, Ayres DL, Darling A, Höhna S, Larget B, Liu L, Suchard MA, Huelsenbeck JP (2012) MrBayes 3.2: Efficient Bayesian Phylogenetic Inference and model choice across a large model space. Systematic Biology 61(3): 539–542. https://doi.org/10.1093/sysbio/sys029

Shimodaira H (2022) An approximately unbiased test of phylogenetic tree selection. Systematic Biology 51(3): 492–508. https://doi.org/10.1080/10635150290069913

Sir EB, Kuhnert E, Surup F, Hyde KD, Stadler M (2015) Discovery of new mitorubrin derivatives from *Hypoxylon fulvo-sulphureum* sp. nov. (Ascomycota, Xylariales). Mycological Progress 14(5): 28. https://doi.org/10.1007/s11557-015-1043-1

Sir EB, Kuhnert E, Lambert C, Hladki AI, Romero AI, Stadler M (2016) New species and reports of *Hypoxylon* from Argentina recognized by a polyphasic approach. Mycological Progress 15(4): 42. https://doi.org/10.1007/s11557-016-1182-z

Sir EB, Becker K, Lambert C, Bills GF, Kuhnert E (2019) Observations on Texas hypoxylons, including two new *Hypoxylon* species and widespread environmental isolates of the *H. croceum* complex identified by a polyphasic approach. Mycologia 111(5): 832–856. https://doi.org/10.1080/00275514.2019.1637705

Smith CL (1893) Some Central American Pyrenomycetes. Bulletin from the laboratories of natural history of the State University of Iowa 2: 408.

Stadler M, Fournier J, Granmo A, Beltrán-Tejera E (2008) The "red Hypoxylons" of the temperate and subtropical Northern hemisphere. North American Fungi 3: 73–125. https://doi.org/10.2509/naf2008.003.0075

Stadler M, Fournier J, Læssøe T, Chlebicki A, Lechat C, Flessa F, Rambold G, Peršoh D (2010) Chemotaxonomic and phylogenetic studies of *Thamnomyces* (Xylariaceae). Mycoscience 51(3): 189–207. https://doi.org/10.1007/S10267-009-0028-9

Stadler M, Kuhnert E, Peršoh D, Fournier J (2013) The Xylariaceae as model example for a unified nomenclature following the "One Fungus-One Name" (1F1N) concept. Mycology 4: 5–21. https://doi.org/10.1080/21501203.2013.782478

Stadler M, Læssøe T, Fournier J, Decock C, Schmieschek B, Tichy H-V, Peršoh D (2014) A polyphasic taxonomy of *Daldinia* (Xylariaceae)1. Studies in Mycology 77: 1–143. https://doi.org/10.3114/sim0016

Stadler M, Lambert C, Wibberg D, Kalinowski J, Cox RJ, Kolařík M, Kuhnert E (2020) Intragenomic polymorphisms in the ITS region of high-quality genomes of the Hypoxylaceae

(Xylariales, Ascomycota). Mycological Progress 19(3): 235–245. https://doi.org/10.1007/s11557-019-01552-9

Surup F, Mohr KI, Jansen R, Stadler M (2013) Cohaerins G-K, azaphilone pigments from *Annulohypoxylon cohaerens* and absolute stereochemistry of cohaerins C–K. Phytochemistry 95: 252–258. https://doi.org/10.1016/j.phytochem.2013.07.027

Surup F, Narmani A, Wendt L, Pfütze S, Kretz R, Becker K, Menbrivès C, Giosa A, Elliott M, Petit C, Rohde M, Stadler M (2018) Identification of fungal fossils and novel azaphilone pigments in ancient carbonised specimens of *Hypoxylon fragiforme* from forest soils of Châtillon-sur-Seine (Burgundy). Fungal Diversity 92(1): 345–356. https://doi.org/10.1007/s13225-018-0412-x

Tang A, Jeewon R, Hyde KD (2009) A re-evaluation of the evolutionary relationships within the Xylariaceae based on ribosomal and protein-coding gene sequences. Fungal Diversity 34: 127–155.

Tamura K, Stecher G, Kumar S (2021) MEGA11: Molecular evolutionary genetics analysis Version 11. Molecular Biology and Evolution 38(7): 3022–3027. https://doi.org/10.1093/molbev/msab120

Tian DS, Kuhnert E, Ouazzani J, Wibberg D, Kalinowski J, Cox RJ (2020) The sporothriolides. A new biosynthetic family of fungal secondary metabolites. Chemical Science 11(46): 12477–12484. https://doi.org/10.1039/D0SC04886K

Triebel D, Peršoh D, Wollweber H, Stadler M (2005) Phylogenetic relationships among *Daldinia*, *Entonaema* and *Hypoxylon* as inferred from ITS nrDNA analyses of Xylariales. Nova Hedwigia 80(1–2): 25–43. https://doi.org/10.1127/0029-5035/2005/0080-0025

U'Ren JM, Miadlikowska J, Zimmerman NB, Lutzoni F, Stajich JE, Arnold AE, U'Ren JM (2016) Contributions of North American endophytes to the phylogeny, ecology, and taxonomy of Xylariaceae (Sordariomycetes, Ascomycota). Molecular Phylogenetics and Evolution 98: 210–232. https://doi.org/10.1016/j.ympev.2016.02.010

Van der Hooft JJJ, Mohimani H, Bauermeister A, Dorrestein PC, Duncan KR, Medema MH (2020) Linking genomics and metabolomics to chart specialized metabolic diversity. Chemical Society Reviews 49(11): 3297–3314. https://doi.org/10.1039/D0CS00162G

Vicente TFL, Gonçalves MFM, Brandão C, Fidalgo C, Alves A (2021) Diversity of fungi associated with macroalgae from an estuarine environment and description of *Cladosporium rubrum* sp. nov. and *Hypoxylon aveirense* sp. nov. International Journal of Systematic and Evolutionary Microbiology 71(2): 004630. https://doi.org/10.1099/ijsem.0.004630

Vilgalys R, Hester M (1990) Rapid genetic identification and mapping of enzymatically amplified ribosomal DNA from several *Cryptococcus* species. Journal of Bacteriology 172(8): 4238–4246. https://doi.org/10.1128/jb.172.8.4238-4246.1990

Vu D, Groenewald M, de Vries M, Gehrmann T, Stielow B, Eberhardt U, Al-Hatmi A, Groenewald JZ, Cardinali G, Houbraken J, Boekhout T, Crous PW, Robert V, Verkley GJM (2019) Large-scale generation and analysis of filamentous fungal DNA barcodes boosts coverage for kingdom fungi and reveals thresholds for fungal species and higher taxon delimitation. Studies in Mycology 92(1): 135–154. https://doi.org/10.1016/j.simyco.2018.05.001

Wang M, Carver JJ, Phelan VV, Sanchez LM, Garg N, Peng Y, Nguyen DD, Watrous J, Kapono CA, Luzzatto-Knaan T, Porto C, Bouslimani A, Melnik AV, Meehan MJ, Liu WT, Crüsemann M, Boudreau PD, Esquenazi E, Sandoval-Calderón M, Kersten RD, Pace LA, Quinn RA, Duncan KR, Hsu CC, Floros DJ, Gavilan RG, Kleigrewe K, Northen T, Dutton RJ, Parrot D, Carlson EE, Aigle B, Michelsen CF, Jelsbak L, Sohlenkamp C, Pevzner P, Edlund A, McLean J, Piel J, Murphy BT, Gerwick L, Liaw CC, Yang YL, Humpf HU, Maansson M, Keyzers RA, Sims AC, Johnson AR, Sidebottom AM, Sedio BE, Klitgaard A, Larson CB, Boya CAP, Torres-Mendoza D, Gonzalez DJ, Silva DB, Marques LM, Demarque DP, Pociute E, O'Neill EC, Briand E, Helfrich EJN, Granatosky EA, Glukhov E, Ryffel F, Houson H, Mohimani H, Kharbush JJ, Zeng Y, Vorholt JA, Kurita KL, Charusanti P, McPhail KL, Nielsen KF, Vuong L, Elfeki M, Traxler MF, Engene N, Koyama N, Vining OB, Baric R, Silva RR, Mascuch SJ, Tomasi S, Jenkins S, Macherla V, Hoffman T, Agarwal V, Williams PG, Dai J, Neupane R, Gurr J, Rodríguez AMC, Lamsa A, Zhang C, Dorrestein K, Duggan BM, Almaliti J, Allard PM, Phapale P, Nothias LF, Alexandrov T, Litaudon M, Wolfender JL, Kyle JE, Metz TO, Peryea T, Nguyen DT, VanLeer D, Shinn P, Jadhav A, Müller R, Waters KM, Shi W, Liu X, Zhang L, Knight R, Jensen PR, Palsson B, Pogliano K, Linington RG, Gutiérrez M, Lopes NP, Gerwick WH, Moore BS, Dorrestein PC, Bandeira N (2016) Sharing and community curation of mass spectrometry data with Global Natural Products Social Molecular Networking. Nature Biotechnology 34(8): 828–837. https://doi.org/10.1038/nbt.3597

Wang F, Liigand J, Tian S, Arndt D, Greiner R, Wishart DS (2021) CFM-ID 4.0: More Accurate ESI-MS/MS Spectral Prediction and Compound Identification. Analytical Chemistry 93(34): 11692–11700. https://doi.org/10.1021/acs.analchem.1c01465

Wendt L, Sir EB, Kuhnert E, Heitkämper S, Lambert C, Hladki AI, Romero AI, Luangsa-ard JJ, Srikitikulchai P, Peršoh D, Stadler M (2018) Resurrection and emendation of the Hypoxylaceae, recognised from a multigene phylogeny of the Xylariales. Mycological Progress 17(1–2): 115–154. https://doi.org/10.1007/s11557-017-1311-3

White TJ, Bruns TD, Lee S, Taylor JW (1990) Amplification and direct sequencing of fungal ribosomal RNA for phylogenetics. In: Innis MA, et al. (Eds) PCR protocols: a guide to methods and applications. Academic Press, San Diego, 315–322. https://doi.org/10.1016/B978-0-12-372180-8.50042-1

Wibberg D, Stadler M, Lambert C, Bunk B, Spröer C, Rückert C, Kalinowski J, Cox RJ, Kuhnert E (2021) High quality genome sequences of thirteen Hypoxylaceae (Ascomycota) strengthen the phylogenetic family backbone and enable the discovery of new taxa. Fungal Diversity 106(1): 7–28. https://doi.org/10.1007/s13225-020-00447-5

Zhang N, Castlebury LA, Miller AN, Huhndorf SM, Schoch CL, Seifert KA, Rossman AY, Rogers JD, Kohlmeyer J, Volkmann-Kohlmeyer B, Sung G-H (2006) An overview of the systematics of the Sordariomycetes based on a four-gene phylogeny. Mycologia 98(6): 1076–1087. https://doi.org/10.1080/15572536.2006.11832635

Zhang D, Gao F, Jakovlić I, Zou H, Zhang J, Li WX, Wang GT (2020) PhyloSuite: An integrated and scalable desktop platform for streamlined molecular sequence data management and evolutionary phylogenetics studies. Molecular Ecology Resources 20(1): 348–355. https://doi.org/10.1111/1755-0998.13096

## Supplementary material 1

**Supplementary information**

Authors: Marjorie Cedeño-Sanchez, Esteban Charria-Girón, Christopher Lambert, J. Jennifer Luangsa-ard, Cony Decock, Raimo Franke, Mark Brönstrup, Marc Stadler

Data type: Alignments and MS raw data (PDF file)

Copyright notice: This dataset is made available under the Open Database License (http://opendatacommons.org/licenses/odbl/1.0/). The Open Database License (ODbL) is a license agreement intended to allow users to freely share, modify, and use this Dataset while maintaining this same freedom for others, provided that the original source and author(s) are credited.

Link: https://doi.org/10.3897/mycokeys.95.98125.suppl1